ISTANBUL TECHNICAL UNIVERSITY ★ GRADUATE SCHOOL OF SCIENCE ENGINEERING AND TECHNOLOGY

PRODUCTION AND CHARACTERIZATION OF ZIRCONUIM BASED BULK METALLIC GLASSESS

M.Sc. THESIS

Doğa BİLİCAN

Department of Metallurgical And Materials Engineering

Production Metallurgy and Technologies Engineering Programme

MAY 2015

ISTANBUL TECHNICAL UNIVERSITY ★ GRADUATE SCHOOL OF SCIENCE ENGINEERING AND TECHNOLOGY

PRODUCTION AND CHARACTERIZATION OF ZIRCONUIM BASED BULK METALLIC GLASSESS

M.Sc. THESIS

Doğa BİLİCAN
506131205

Department of Metallurgical and Materials Engineering

Production Metallurgy and Technologies Engineering Programme

Thesis Advisor: Assoc. Prof. C. Bora DERİN

MAY 2015

İSTANBUL TEKNİK ÜNİVERSİTESİ ★ FEN BİLİMLERİ ENSTİTÜSÜ

ZİRKONYUM ESASLI KÜTLESEL METALİK CAMLARIN ÜRETİMİ VE KARAKTERİZASYONU

YÜKSEK LİSANS TEZİ

Doğa BİLİCAN
506131205

Metalurji ve Malzeme Mühendisliği Bölümü

Üretim Metalurjisi ve Teknolojileri Mühendisliği Programı

Tez Danışmanı: Doç. Dr. C. Bora DERİN

MAYIS 2015

Doğa BİLİCAN, a M.Sc. student, of ITU Graduate School of Science, Engineering and Technology, 506131205, successfully defended the thesis entitled "Production and Characterization of Zirconium-based Bulk Metallic Glasses", which she prepared after fulfilling the requirements specified in the associated legislations, before the jury whose signatures are below.

Thesis Advisor :	**Assoc. Prof. C. Bora DERİN** İstanbul Technical University	.....
Jury Members :	**Assoc. Prof. Mustafa BAKKAL** İstanbul Technical University	.....
	Assoc. Prof. Derya DIŞPINAR İstanbul University	.....

Date of Submission : 4 May 2015
Date of Defense : 27 May 2015

To my mother,

FOREWORD

First of all, I would like to express my gratitude to my thesis advisor Assoc. Prof. C. Bora DERİN for his support, kindness and patience through my studies.

I am also grateful to Dr. Murat ALKAN, Dr. Hakan MORCALI and research assistant Mehmet BUĞDAYCI for being helpful to me in anything that I have asked for.

I also would like to thank to Assoc. Prof. Mustafa BAKKAL and research assistant Azmi TİMUR for guiding me throughout the experimental studies I am supposed to follow.

I would like to thank to Dr. Yunus BAŞ for assisting me at my studies in BOREN.

I would like to thank to specialist İnci KOL for her help in chemical analyses.

I would like to thank to research assistant Faiz MUHAFFEL, Dr. Erdem ŞEŞEN, Burak Yalçın and Sevinch RAHİMİ for their help in metallography.

Lastly, I am also truly grateful to my family for their support and patience they show throughout my undergraduate and graduate studies.

May 2015 Doğa BİLİCAN

TABLE OF CONTENTS

ABBREVIATIONS

XRD	: X-ray Diffractometry
TEM	: Transmission Electron Microscopy
SEM	: Scanning Electron Microscopy
DTA	: Differential Thermal Analysis
DSC	: Differential Scanning Calorimetry
nm	: Nanometer
mm	: Milimeter
BMG	: Bulk Metallic Glass
$\mathbf{T_g}$	: Glass Transition Temperature
$\mathbf{T_m}$	: Melting Temperature
$\mathbf{T_{rg}}$	: Reduced Glass Transition Temperature
$\mathbf{T_l}$	: Liquiduous Temperature
GFA	: Glass Forming Ability
X	: Crystallization Fraction
$\boldsymbol{R_c}$	: Critical Cooling Rate
TTT diagram	: Time – Temperature – Transformation diagram
K/min	: Kelvin per minute
$\mathbf{Ks^{-1}}$	: Kelvin per second
ppm	: Part per million
appm	: Atomic part per million
K	: Kelvin
MPa	: Megapascal
kPa	: Kilopascal
V	: Volt
Hz	: Heartz
$\mathbf{^oC}$	: Celsius
A:	: Ampere

LIST OF TABLES

Page

LIST OF FIGURES

Page

PRODUCTION AND CHARACTERIZATION OF ZIRCONIUM BASED BULK METALLIC GLASSES

SUMMARY

In this study Vit105, which has Zr52.5Ti5Ni14.6Cu17.9Al10 as its atomic ratio, a commercial bulk metallic glass alloy which consists of non-toxic metals apart from exhibiting high mechanical and corrosion properties, was synthesized by using Edmund Bühler Arc melting and Suction Casting Equipments. The experiments were carried out in high purity argon atmosphere with high vacuum values up to 10^{-6} mbar by arc melting along with Ti- and Zr- getters. As starting materials, in order to observe the differences in results based on them, Zr bar with 99.5% purity and Zr lumps with 99.8% metal basis containing Hf up to 3-4% were used along with other high purity components in order to examine the increase in entropy because of having Hf in the alloy on glass formation.

As oxygen impurity avoids glass formation, in order to suppress the nucleating effect of it, oxygen scavenging effect of yttrium by microalloying depending on the fact that it has a higher oxygen affinity than the other components by having it included in 0.3 at.%, 0.8 at. %, 0.6Y%,at. % 0.7 at. ratios were studied.

Depending on visual inspections, it was seen that shiny and lustrous which indicate glass formation were obtained for all samples.

In the XRD analyses carried out, phase composition of surface and inner parts of the samples were examined. For sample preparation, the samples were cut by SiC and diamond cutters horizontally in order to search the effect of rapid solidification by detecting phases formed on the surface that was in contact with the copper crucible, the center and the upper surface of the sample. According to the results obtained, amorphization was seen to increase in the central region compared to surface parts of the samples. Also, it was seen that in rod sample, as cooling is provided homogeneously throughout the entire structure, crystallization could more successfully be prevented and make the glassy phase become formed.

Following sample prepation steps which consisted of grinding, polishing and etching respectively, the optical microscopy studies with 100 times magnification was implemented. As a result of this, the effect of microalloying with yttrium was seen to prevent dendrite formation in the structure and depending on different amounts of addition as it decreases the nucleating effect of oxygen presence by combining oxygen to itself in Y_2O_3 form, a compound that suppresses heterogeneous nucleation, which tends to make the composition lead to partial amorphization.

ZİRKONYUM ESASLI KÜTLESEL METALİK CAMLARIN ÜRETİMİ VE KARAKTERİZASYONU

ÖZET

İleri teknoloji malzeme geliştirme çalışmaları 20. yüzyılın ikinci yarısının temel araştırma odaklarından biri olmuştur. Termodinamik denge esas alınarak yapılan klasik metalurji çalışmalarının yanı sıra metalik malzemelerde denge-dışı fazlar hakkında çalışmalara olan yönelmeler yeni bir araştıma alanının oluşmasını sağlamıştır.Metal alaşımı eriyiğini hızlı soğutma ilkesi temel alınarak amorf faz elde etme prensibine dayalı geliştirilen yöntemler önce ince film formunda, daha sonra kütlesel üretimlerine olanak tanımıştır.

En az 1 mm çapta, silindir şeklinde amorf fazda sentezlenebilen metal alaşımları kütlesel metalik camlar olarak adlandırılmaktadır. Silindir şeklinde sentezlenebilme boyutları bu bileşimlerin camlaşma eğilimini göstermektedir. Teorik bir temelden çok deneme yanılma yöntemine dayalı olarak yapılan çalışmalar metal alaşımlarında camlaşmanın genel olarak üçten fazla farklı atomik çap büyüklüklerine sahip ve olabildiğinde negatif bir karışım entalpisine sahip sistemler oluşturularak sağlandığı görülmüştür. Yapılan çalışmalar kütlesel metalik cam sentezinde alaşım bileşiminin önemini ve sentezlenen ortamda bulunan oksijenin kontamine edici etkisini ortaya koymuştur.

Metal alaşımlarındacamlaşma öncelikle soy metal esaslı alaşımlarda sağlandıktan sonra zirkonyum, bakır ve demir esaslı gibi pek çok sistemde sağlanmıştır. Bunlardan zirkonyum esaslı kütlesel metalik camlar, Vitreloy serisi adı altında düşük kritik soğuma hızları ile ticari boyutta ilk sentezlenebilen kütlesel metalik cam serisini oluşturmuştur.

Bu çalışmada $Zr_{52.5}Ti_5Ni_{14.9}Al_{10}$atomik bileşimine sahip, bileşiminden toksik metal bulundurmaman yanı sıra üstün mekanik ve korozon dayanımı özellikleri gösteren, ticari bir kütlesel metalik cam malzemesi Vit105 üretilmesi amaçlanmıştır. Numunelerin sentezlenmesi için Edmund Bühler Ark ile Ergitme ve Emme Döküm cihazlarından faydalanılmıştır. Deneyler, 0.7 ve 0.5 bar yüksek safiyet argon atmosferinde, 10^{-6} mbar a varan yüksek vakum düzeylerine varılabilen ortamlarda, Ti- ve Zr- oksijen gidericiler yardımıyla gerçekleştirilmiştir. Başlangıç malzemesine bağlı farkların camlaşmadaki etkisini göstermek için, diğer yüksek safiyet metallerle beraber %99.5 safiyette Zr kristal bar ve % 99.8 metal esaslı Zr (%3-4 Hf hariç) yumrular kullanılmıştır. Yapıda Hf bulunmasının neden olduğu entropi değişiminin amorflaşmadaki etkisi incelenmiştir.

Vakumlu ortamda ark ile ergitme yöntemi ilemetal alaşımları elde etmek için sıklıkla kullanılan bir yöntemdir. Ar atmosferinde gerçekleştirilen işlemde hızlı soğumanın etkisini verimli bir şekilde göstermesi için bakır numune içinden su kanalları geçen bakır potalarda gerçekleştirilir. Numunelerde homojen bir ergime sağlamak için ters yüz edilerek tekrar ergitme uygulanır. Ark ile ergitmeyi takiben uygulanan emme döküm ise, numunenin bulunduğu ortamda belli bir basınç varken, eriyik haldeki numuneyi tamemen Vakuma alınmış bir ortama basınç farkı dolayısıyla geçişi sağlanarak gerçekleştirilir. Bu çalışmada ark ile ergitme ile hazırlanan buton şeklindeki numunelerin yanı sıra bu metodla hazırlanan 3 mm çapında ve 6 cm uzunluğunda silindir şeklindeki numunelere yer verilmiştir.

Ark ile ergitmede oluşturulan sıvı eriyikten hızlı bir soğutma ile ısı ekstrakte edilmesinin amorflaşmayı sağlaması, katılaşmanın başlamasına dayalı oluşan katı/sıvı arayüzeyinin ilerlemesinin durdurulmasına dayanır. Bunun bir sonucu olarak amorflaşma genel olarak numunenin alt ve üst yüzeylerinde değil merkeze doğru sağlanabilmektedir. Ayrıca, numunenin bakır potaya temas eden yüzeyi devamlı soğumaya maruz kaldığı için tam erime o bölgede hiç bir zaman gerçekleşmemektedir. Emme dökümle elde edilen silindir numunelerde ise her yönden eşit soğuma elde edildiği için daha başarılı bir amorflaşma elde edimektedir.

Kütlesel metalik cam sentezlerinde camlaşmayı desteklediği ortaya konulan belli başlı parametreler sistemlerin soğuma hızı, indirgenmiş cam geçiş sıcaklığı, derin ötektik oluşumu ve mikroalaşımlamadır. Bir metal alaşımı sistemi için çizilen TTT diyagramındaki C eğrisine teğet olarak çizilen eğrinin eğimiyle belirlenen kritik soğuma hızı camlaşmadaki temel parametredir. Cam geçiş sıcaklığının liküdüs sıcaklığına oranı ile belirlenen indirgenmiş cam geçiş sıcaklığı ile camlaşma eğilimi metalik cam sistemlerini belirlemede bir diğer etkendir. Metallerin ayrı ayrı ergime noktalarıyla bir arada sıvı halde bulunabildikleri ötektik sıcaklıkları arasındaki farkın yüksek olmasına dayalı olarak oluşan ötektikler derin ötektik kabul edilmektedir. Derin ötektik oluşumunun hızlı soğutmayla beraber ötektik altı veya üstü alaşımlara göre daha iyi camlaştığı gözlemlenmiştir. Bunlara ilaveten camlaşabilen sistemlerdeki bu eğilimi artırmak için yapılan küçük ve büyük boyutlardaki farklı metal atomlarıyla yapılan mikroalaşımlamaların verimli sonuçlar sağladığı görülmüştür.

Tam olarak mekanizması bilinmemekle beraber metalik camlarda mikroalaşımlama ile camlaşma eğiliminin artırılmasının küçük boyutlu atomların metal kümelerinin boşluklarını doldurarak amorf matriksi serbestleştirdikleri görülmüştür. Büyük çaptaki atomlarla yapılan ilavelerle ise daha çok eriyikteki oksijenin bileşime yapılan ilave metale bağlanarak amorf matriksten uzaklaştırılmıştır.

Zirkonyum esaslı kütlesel metalik camlarda bu konuda yapılan çalışmalar Y, Sc ve La mikroalaşımlamaları ile olumlu sonuçlar vermiştir. Ancak ilave miktarına göre amorflaşmanın yanı sıra farklı kristal piklerin oluşumu gözlemlenmiştir.

Oksijen empüritesi camlaşmayı önlediğinden, oluşturduğu çekirdeklenme etkisinin önüne geçmek için, ıtriyum elementinin mikroalaşımlama ile oksijen ile reaksiyona girip, yapıda heterojen çekirdeklenmeyi önleyen Y_2O_3 formunda çökelmesi ve amorf matriksi serbest bırakma özelliğinden kaynaklanır. Bunu sağlayan özelliği yapıdaki diğer tüm bileşenlerden daha yüksek oksijen afinitesine sahip olmasıdır.Ayrıca ıtriyum liküdüs çizgisinde bu özelliğiyle düzenli bir atom kümeleşmesi oluşturarak hızlı soğutmanın daha iyi bir amorflaşma gerçekleştirmesini sağlar. Bu çalışmada

kullanılan bileşimler ıtriyum atomca %0.3, %0.8, %0.6 ve %0.7 oranında bileşime dahil edilerek çalışılmıştır.

Görsel olarak tüm numunelerde, metalik camların genel özelliği olan parlak bir yüzey elde edilmiştir.BazıNumunelerde soğuma esnasında çatlak oluştuğu görülmüş, bu durum kristalizasyon işareti olduğundan numuneler yeniden ergitilerek bu durumun üstesinden gelinmeye çalışılmıştır. Oluşan çatlakların oldukça gevrek bir yüzeye sahip olmaları yeterli hızlı soğutma sağlanamadığında amorflaşma gerçekleşemediğinden sistemdeki yüksek entropinin neden olduğu gerilmelerdir.

FactSage 6.4 yazılımı ile gerçekleştirilen ergime sıcaklığı hesaplamasında sistemin 785.9 ^{o}C'de tamamen sıvı faza geçtiği görülmüştür. Bileşimde alüminyumun diğerlerine göre daha düşük olan 660 C ergime sıcaklığı değerinden ötürü stokiometrik oranda dahil edilmesi mümkün olamadığından kütlece yaklaşık %35 daha fazla oranda bileşime dahil edilerek atomca bileşim oranı tam olarak elde edilebilmiştir. Bu durum atomik absorpsiyon analizi ile doğrulanmıştır. Gerçekleştirilen oksijen analizi ile numunelerin açık atmosferde muhafaza edilen toz formdaki başlangıçç malzemeleri yerine argon atmosferi altında muhafaza edilen başlangıç malzemeleriylle çalışılması gerektiği ortaya konularak bu şekilde devam edilmiştir.

Ark ile ergitme ile hazırlanan kütlesel metalik camlarda numunelerin alt ve üst yüzeylerinin XRD analizleri kristal pikler içerirken enine kesitlerde amorflaşma görüldüğünden numunelerin iç bölgesinin incelenmesi amaçlanmıştır.

Yapılan XRD çalışmalarında, numunelerin yüzeyleri ve merkezlerindeki mikroyapıları incelenmiştir. Numune hazırlamada SiC kesiciden faydalanılarak numuneler ikiye kesilmiştir. Hızlı soğutmanın bakır yüzey ile temasta olan üzeyinde, merkezinde ve üst yüzeyinde olan fazlar incelenmiştir. Elde edilen sonuçlar amorflaşmanın merkezde yüzeylere göre daha yüksek olduğunu göstermiştir. Ayrıca çubuk numunelerde, soğuma tüm yüzey boyunca eşit düzeyde sağlanabildiğinden kristalizasyonun daha başarılı şekilde önüne geçilmiştir.

Geleneksel döküm alaşımlarında optik mikroskopide numune yüzeyinden merkeze doğru görülen çil bölgesi, kolonsal yapı, eşeksenli taneler bölgesi; kütlesel metalik camlarda eşeksenli taneler bölgesinin yerine amorf bölge görülmesinin haricinde geleneksel döküm alaşımlarıyla paralellik gösterir. Bu nedenle bu metodla inceleme yapabilmek için numunenin kesitinden faydalanmak gerekir.

Optik mikroskopi çalışmaları, sırasıyla zımparalama, parlatma ve dağlama aşamalarından sonra 100 kat büyütme ile 10 mikron büyüklüğündeki incelenerek gerçekleştirilmiştir. Bunun sonucunda ıtriyum ilaveli numunelerde dendrit oluşumunun önüne geçildiği görülmüştür. Değişen ıtriyum miktarı ilavesine göre ıtriyumun oksijeni kendine bağlayarak sıvı alaşımdaki serbest oksijeni azaltıp çekirdeklenmenin önüne geçmesinin kısmi amorflaşmaya olanak sağladığı görülmüştür.

1. INTRODUCTION

Because of the continuous quest in advanced materials field, along with the rapid progress in technology in the last 50-60 years and the future demands in materials science, bulk metallic glasses has become a hot topic as this group of materials possess stronger, stiffer and lighter properties compared to conventional metallic materials besides higher mechanical and anti-corrosive properties. been the major preoccupation of materials scientists during the past several years. Recent investigations have focused on the improvement of the properties and performance of existing materials and/or synthesizing and developing completely new materials. Noteworthy enhancements were achieved in the mechanical, chemical, and physical properties of materials by the addition of alloying elements, microstructural modification, and by subjecting the materials to thermal, mechanical, or thermo-mechanical processing methods.

Apart from processes that are implemented atequilibrium conditions, search for novel advanced materials has made attracted attention to execute research studies focused on processes that can be developed at nonequilibrium conditions. This approach made it possible for designin several nonequilibrium processing techniques such as rapid solidification processing (RSP), mechanical alloying, plasma processing, vapor deposition, and spray deposition. The process of "energize and quench" which is realized to produce metastable materials, suggested by Turnbull (1981) has been the basis of nonequilibrium studies.

In rapid solidification method, a molten metal or alloy is solidified very rapidly at rates of about 10^6 K s^{-1}, but at least at about 10^4 K s^{-1}. The metastable materials obtained by this method were seen to show improved physical, chemical, and mechanical characteristics in comparison to their conventional materials. To have the fact that the structure metallic materials, which are crystalline by nature could be turned into amorphous has been the key point for the metallic glasses become a major research topic for novel materials. Following thin film synthesis studies, having them cast in bulk forms has initiated bulk metallic glasses studies become

accepted as a unique topic. As the research in this field went on mostly based on trial and error methods in the beginning period of it, it has been clarified that designing multicomponent alloy compositions with constituents that have different atomic radii, low enthalpy of mixing and usage of high purity metals as starting materials made glass formation probable. As a simple and widely applicable method, arc melting and suction casting have emerged as methods that are utilized for bulk metallic glass casting as well as conventional metallic alloys (Inoue and Suryanarayana, 2011). Phase analysis for these materials include XRD, optical microscopy, back scattered SEM, TEM and thermal analysis methods such as DSC and DTA.

Among all metallic alloys, zirconium based alloys have been evaluated to be the ones that are most liable to be obtained in bulk metallic glass form depending on their high cooling rates. On account of that fact, a series of bulk metallic glasses are being produced commercially with the brand name "Vitreloy series". Among them Vitreloy105 (Vit105) which has $Zr_{52.5}Ti_5Ni_{14.6}Cu_{17.9}Al_{10}$ as its chemical formula, outstands as a novel bulk metallic glass which has as it totally consists of non-toxic metals and has a significantly low cooling rate of approximately 10 K s^{-1}(Telford, 2004). However as their high affinity for oxygen acts as a hindering factor when it comes to glass formation, studies based on microalloying Zr-based alloys with metals that have higher oxygen affinities than that of zirconium and having crystallization suppressed throughout the glass matrix as a result of having oxygen combined to the microalloyed metal, is a method that many research studies have been concentrated on (Kündig, 2002).

In this study, it was aimed to produce $Zr_{52.5}Ti_5$Ni14.6Cu17.9Al10 alloy by arc melting and suction casting method. Apart from high purity zirconium crystal bar as the starting material, zirconium lumps that include hafnium are used as well in order to observe the effect of increase in entropy on glass formation. Besides, yttrium is included as a component by microalloying to examine the effect of it as an oxygen scavenger. The effects of increased entropy and oxygen scavenging in the microstructure are studied by XRD and metallography studies.

In rapid solidification method, a molten metal or alloy is solidified very rapidly at rates of about 10^6 K s^{-1}, but at least at about 10^4 K s^{-1}. The metastable materials obtained by this method were seen to show improved physical, chemical, and

mechanical characteristics in comparison to their conventional materials. To have the fact that the structure metallic materials, which are crystalline by nature could be turned into amorphous has been the key point for the metallic glasses become a major research topic for novel materials. Following thin film synthesis studies, having them cast in bulk forms has initiated bulk metallic glasses studies become accepted as a unique topic. As the research in this field went on mostly based on trial and error methods in the beginning period of it, it has been clarified that designing multicomponent alloy compositions with constituents that have different atomic radii, low enthalpy of mixing and usage of high purity metals as starting materials made glass formation probable. As a simple and widely applicable method, arc melting and suction casting have emerged as methods that are utilized for bulk metallic glass casting as well as conventional metallic alloys (Inoue and Suryanarayana, 2011). Phase analysis for these materials include XRD, optical microscopy, back scattered SEM, TEM and thermal analysis methods such as DSC and DTA.

Among all metallic alloys, zirconium based alloys have been evaluated to be the ones that are most liable to be obtained in bulk metallic glass form depending on their high cooling rates. On account of that fact, a series of bulk metallic glasses are being produced commercially with the brand name "Vitreloy series". Among them Vitreloy105 (Vit105) which has $Zr_{52.5}Ti_5Ni_{14.6}Cu_{17.9}Al_{10}$ as its chemical formula, outstands as a novel bulk metallic glass which has as it totally consists of non-toxic metals and has a significantly low cooling rate of approximately 10 K s^{-1} (Telford, 2004). However as their high affinity for oxygen acts as a hindering factor when it comes to glass formation, studies based on microalloying Zr-based alloys with metals that have higher oxygen affinities than that of zirconium and having crystallization suppressed throughout the glass matrix as a result of having oxygen combined to the microalloyed metal, is a method that many research studies have been concentrated on (Kündig, 2002).

In this study, it was aimed to produce $Zr_{52.5}Ti_5Ni_{14.6}Cu_{17.9}Al_{10}$ alloy by arc melting and suction casting method. Apart from high purity zirconium crystal bar as the starting material, zirconium lumps that include hafnium are used as well in order to observe the effect of increase in entropy on glass formation. Besides, yttrium is included as a component by microalloying to examine the effect of it as an oxygen

scavenger. The effects of increased entropy and oxygen scavenging in the microstructure are studied by XRD and metallography studies.

2. LITERATURE REVIEW

2.1 Definition of glass

Glass is described as an amorphous solid that lacks in long range order and is formed by continuous hardening of a cooled liquid. What distinguishes glass from solid is a viscosity value of 10^{13} poise. The characterization of amorphous structure is carried out by X-ray diffraction (XRD), transmission electron microscopy (TEM) and thermal analysis(DTA and DSC). A solid will be called amorphous, when no long range order can be detected down to approximately 2 nm (Peker, 1994; Mei, 2009; Suryanarayana and Inoue, 2011).

2.2 Glass Transition

Glass is a liquid that has lost its ability to flow. Upon cooling to temperatures below its melting point, a liquid can solidify as a crystal or form a glass. Thermodynamically, a periodic crystal has lower energy compared to glass. However, in some cases, the liquid atoms can easily assemble into non-crystalline packing modes, especially when the time available to form a periodic structure becomes a factor. A liquid cooled below its melting point does not crystallize spontaneously because of an activation barrier to nucleation which arises from the competition between volume and interfacial free energies. The level of undercooling depends on the height of the activation barrier. Figure 2.1 schematically shows the cooling curves for three different levels of undercooling. In case (a), the liquid undercools a little until nucleation is triggered and the liquid is raised to the melting temperature. This is followed by isothermal crystallization until all of the liquid is transformed into crystal. In case (b), the liquid is hypercooled, i.e., the amount of heat released is not enough to raise the sample to the melting temperature from such a deeply undercooled state. In the extreme case as shown by curve (c), the liquid bypasses crystallization completely and passes through glass transition, at which point it falls out of equilibrium and becomes solid-like(Mukherjee, 2005). The glass

transition can be defined as a transition which occurs as a result of having undercooled liquid configurationally freeze into a solid in a rather well defined temperature range during continuous cooling (Peker, 1994).The glass transition temperature is not a constant 2 of the material, but rather is a function of experimental conditions. The slower the cooling rate, the lower will be the value of the glass transition temperature (Mukherjee, 2005).

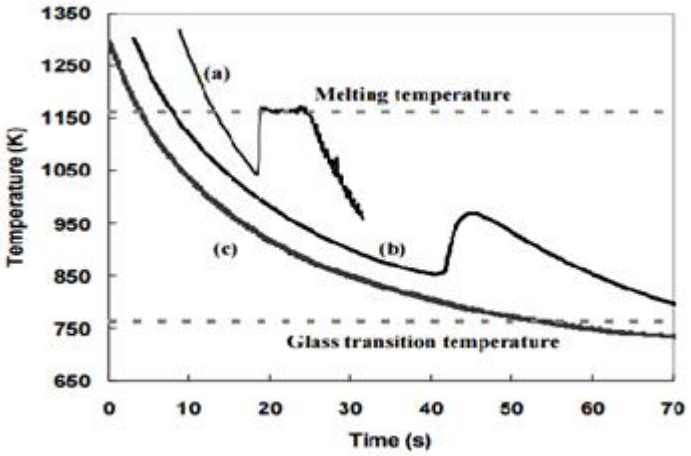

Figure 2.1: Cooling curves showing (a) undercooling followed by isothermal crystallization, (b)hypercooling and (c) vitrification. The melting and glass transition temperatures are shown by the dotted lines (Mukherjee,2005).

An undercooled liquid transforms into a glass during the glass transition as well. This transition can be accepted as reversible neglecting the fact that there might remain irreversible relaxation effects in the glass. During glass transition the atomic mobility, which is related to the viscosity, changes by several orders of magnitude. In figure 2.2 (a) the temperature dependence of the viscosity of an undercooled liquid is shown schematically. In general, the glass transition takes place in a relatively small temperature interval though it is dependent on the rate of heating and cooling. The glass transition temperature, Tg is defined as the temperature at which viscosity has a value of 10^{13} poise. As a significant parameter for glass formation,the reduced glass transition temperature Trg, corresponds to as Trg = 'Tg/Tm, where Tm is the thermodynamic freezing temperature of liquid (where the liquid freezes to the equilibrium crystalline phase(s) (Peker, 1994).

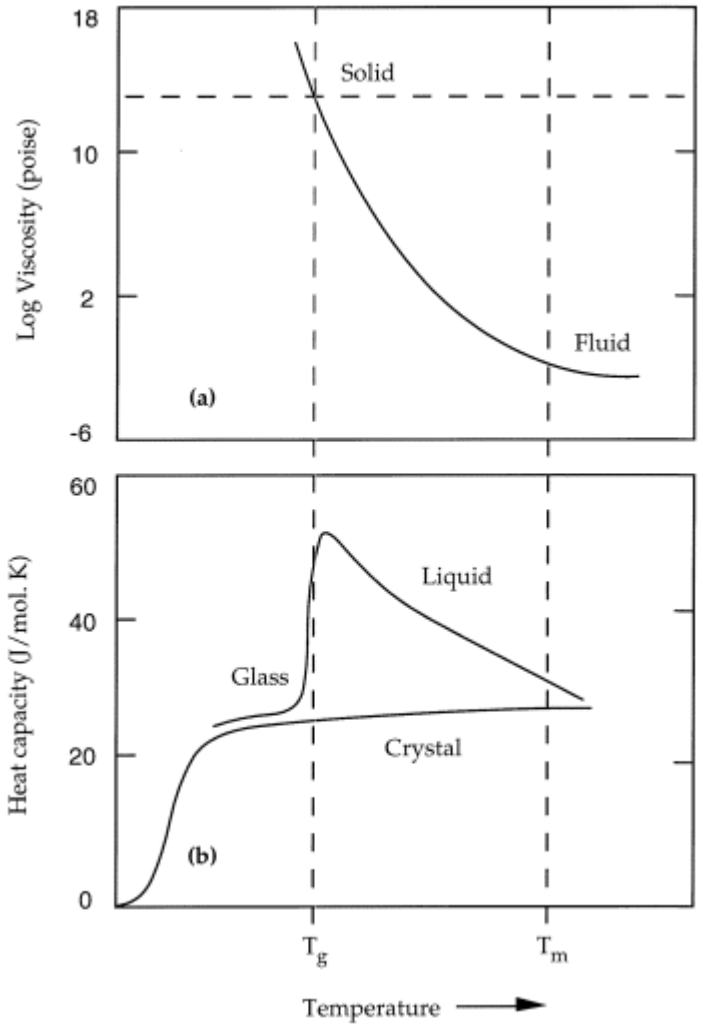

Figure 2.2: (a)Temperature dependence of the viscosity of an undercooled melt.(b)Heat capacity of an undercooledmeltas a function of temperature (Peker, 1994).

2.3 Metallic Glass Formation

Any amorphous alloy with excellent mechanical properties, produced by cooling an alloy melt below the so-called glass transition temperature Tg at a cooling rate below the so-called critical cooling rate is classified as metallic glass. However in case a metallic glass could be synthesized with a diameter > 1mm when cast as a cylinder it is categorized as a bulk metallic glass (BMG). The minimum dimension of the largest sample that can be made fully glassy is named as glass forming ability (GFA). The main rules to obtain a BMG with a high GFA is having;

–a multicomponent system with three or more elements;

–a significant difference of at least 12% in atomic size ratios among the main constituent elements;

– a negative heat of mixing of the components (Fredriksson and Akerlind, 2012).

2.4 Glass Forming Ability

To produce metallic glasses in a reasonable and reliable way, and also to produce them in large quantities and in a reproducible way, it is essential that we understand the basic reasons about glass formation from the liquids. There has been reasonable success in predicting the compositions and alloy systems in which glasses could be synthesized during the 1970s and 1980s. But, with the discovery of bulk metallic glasses (BMGs), the activity in this area has been at a high level in recent times. Both the alloy systems and their compositions, which are likely to be transformed into the glassy condition, have been predicted. The ability of a metallic alloy to transform into the glassy state is defined in this chapter as the glass-forming ability (GFA). (Suryanarayana and Inoue, 2011)

2.4.1 Critical cooling rate

In order to achieve glass formation, detectable crystal nuclei formation which is assumed to have a volume fraction of 10^{-6} must be prevented. This case can only occur if a successfull undercooling of liquid alloy below glass transition temperature T_g is achieved (Suryanarayana and Inoue, 2011).

In case an alloy melt is solidified from a temperature higher than the liquidus temperature, T_l to a temperature lower than the glass transition temperature, Tg, then the volume fraction of the solid crystalline phase, X formed under non-isothermal crystallization conditions is expressed by the following equation (Suryanarayana and Inoue, 2011):

$$X(T) = \frac{4\pi}{3xR^4}\int_{T_l}^{T_g} I(T')\left[\int_{T_l}^{T_g} U(T'')dT''\right]^3 dT' \qquad \textbf{(2.1)}$$

I and U represent the steady-state nucleation frequency and crystal growth rate, respectively. If the volume fraction of the crystalline phase formed is selected as a very small value, say $X = 10^{-6}$, which is accepted as glass formation condition, then the critical cooling rate, R_c can be derived from the equation above such as (Suryanarayana and Inoue, 2011):

$$R_c^4 = \frac{4\pi}{3x10^{-6}} \int_{T_l}^{T_g} I(T') \left[\int_{T_l}^{T_g} U(T'')dT'' \right]^3 dT' \quad \textbf{(2.2)}$$

Due to the fact that *I* and *U* componentsare related to viscosity of the supercooled liquid, η, entropy of fusion, ΔS_f, etc., the critical cooling rate, *R*c decreases with increasing η, ΔS_f, and decreasing liquidus temperature, T_l. The most effective way to determine *R*c is by constructing the time–temperature– transformation (*T*–*T*–*T*) diagrams (Suryanarayana and Inoue, 2011) .

2.4.2 T-T-T diagrams

A schematic time–temperature–transformation (T–T–T) diagram for a hypothetical alloy is shown in figure 2.3.

The temperature is represented on the Y-axis and the time on the X-axis. Since the time required for the transformation to be completed is usually very long, the time is plotted on a logarithmic scale.

The transformation curve, which has a C-shape, represents, at any given temperature, the time required to start the formation of the stable (crystalline) solid phase.

Liquid phase stability is the primary criterion to be taken into consideration for glass forming liquids. It should include two aspects:

(1) the stability of the liquid at the equilibrium state (i.e., stable state)
(2) the stability of the liquid during undercooling (i.e., metastable state).
Assuming that two glass forming liquids have the same *T*g but different T_l, their relative liquid phase stability is then dominated by the stability of their stable states (i.e., the values of T_l).

How stable the liquid phase is to be is determined by how low its T_l value is. In the case that two liquids have the same T_l but different *T*g, their relative liquid phase stability is then dominated by the stability of their metastable states (i.e., the *T*g values). The one with the lower Tg value has a more stable liquid phase.

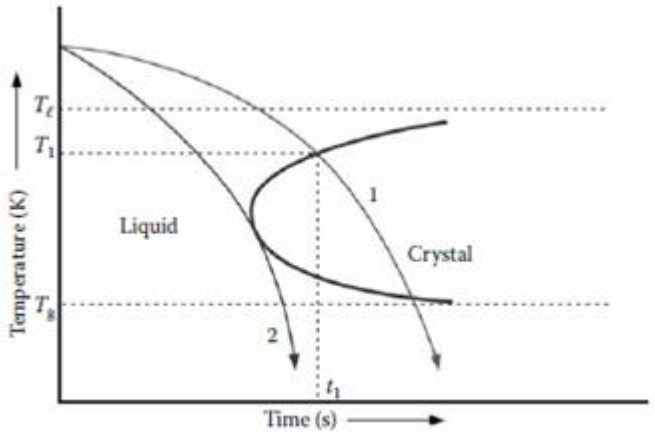

Figure 2.3: T-T-T diagram(Suryanarayana and Inoue, 2011).

In order a crystalline solid structure to be formed, solidification requires quite a long duration. If the alloy is cooled from the liquid state under equilibrium conditions, this case is achieved. Even if the liquid alloy is cooled a little more rapidly solidification occurs at a temperature T_1 and time, t_1, and the product is still a crystalline solid as shown in Figure 2.3. Solidification at higher rates is to cause alike results. However, if the liquid alloy becomes solidified at a rate higher than the cooling rate represented by curve "2"(Fig 2.3), which represents a tangent to the C-curve at its nose, (i.e., the temperature at which the formation of a crystalline phase takes place in the shortest time) crystal formation does not take place at all. Consequently, the liquid will be kept in the supercooled (or undercooled) condition. Assuming that the temperature of this supercooled liquid is decreased more, the viscosity of it will continue to increase up to 10^{12} Pa, the typical solid state viscosity value. The supercooled liquid gains a frozen-in structure and glassy phase is formed at temperatures below Tg. The cooling rate shown by curve "2" in figure 2.3 is called as the "critical cooling rate," and is symbolized as Rc.

What is particularly important about glass transition temperature is that formation of a complete glass form is achieveable in case the liquid alloy is cooled above this rate assuming that it is cooled below Tg. If two liquids have different T_l and T_g, then their liquid phase stability has to be measured by $(1/2)(T_g + T_l)$. The lower this value, the higher the glass forming ability is (Miller and Liaw, 2008).

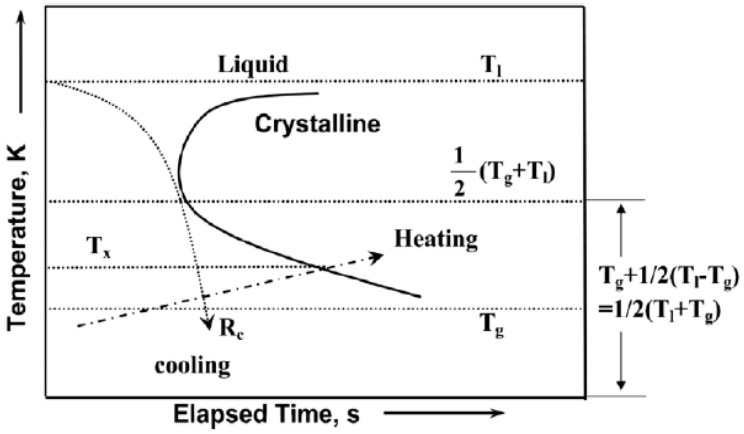

Figure 2.4: T-T-T diagram – The relationship between T_g and T_l (Miller and Liaw, 2008).

However, it is not possible to form a homogeneous glassy phase providing that the cooling is carried out at a rate lower than the critical cooling rate. Providing a cooling rate faster than Rc and a final temperature lower than Tg is the most suitable approach to obtain glass formation. The T-T-T curve and the temperature and time at the nose are determined by the increasing driving force for nucleation as a result of increased supercooling and decreased atomic mobility due to lowering of temperature. By performing the calculations for continuous cooling transformation behavior, Barandiaran and Colmenero(1981) ;

$$lnR = A - \frac{B}{(T_l - T_{xc})^2} \qquad \textbf{(2.3)}$$

where R is the cooling rate, A and B are constants, T_ℓ is the liquidus temperature, T_{xc} is the onset temperature of solidification upon cooling at a rate R. The undercooling ΔT_c ($=T_\ell - T_{xc}$), at which the derivative of transformed fraction, X with respect to temperature, T is a maximum, varies with the cooling rate. As ΔT_c increases to infinity, no crystallization occurs and A=ln R_c. The critical cooling rate, Rc will be obtained by an extrapolation of the fitting of experimental values with the equation. A method like this has been used by others also to estimate R_c by measuring the values of T_l and T_{xc} at a given cooling rate.

Another equation to calculate the critical cooling rate, R_c (K s^{-1}) required for forming a glassy structure from the liquid is as follows d is the sample dimension (e.g., diameter or thickness) in cm:

$$R_c = \frac{10}{d^2} \quad \textbf{(2.4)}$$

Apart from these methods, detection of R_c is also possible using thermal analysis methods such as DSC and DTA (Suryanarayana and Inoue, 2011) .

Rc differs from one alloy system to another. It also differs for different compositions within an alloy system. An extremely high R_c for glass formation in pure metals is needed (typically $>10^{10} - 10^{12}$ K s^{-1}). Depending on the increase in the number of components in the alloy system, the value of R_c is to decrease to 10^2K s^{-1} or less. As BMGs are mostly multicomponent systems, it is possible to have them cast into the glassy state at relatively low R_c values. Very low critical cooling rates of 1.3 . 10−2 K s−1 for a $Pd_{37.5}Cu_{32.5}Ni_{10}P_{20}$ alloy (Nishiyama and Inoue, 2002) and 0.067 K s−1 for a $Pd_{30}Pt_{17.5}Cu_{32.5}P_{20}$ alloy (Nishiyama, Takenaka and Inoue, 2006) have been reported to be sufficient to form BMGs. (Suryanarayana and Inoue, 2011)

2.4.3 Effect of alloying elements

In order to obtain phase transformations at longer times for an alloying system, attempting to shift C-curve of the T-T-T diagrams to the right by elemental composition changes is a commonly applied method. Keeping the liquid in the supercooled condition for a longer period of time is possible in case the C-curve for the liquid-solid transformation is shifted to the right. Consequently, a lower value of Rc for glass formation is obtained.The effect of alloying elements on the required critical cooling rate for glass formation is shown schematically in Figure 2.5.

There are particular ways to determine the solidification rate: As the cooling rate is going to be the highest on the surface of the sample that is in contact with the heat sink, observing the section thickness provides data about the solidification rate. In general, it is expected to have lower solidification rates at the inner region of the material. As a consequence of this, R_c is higher at the surface which results in a higher glass formation at the surface.

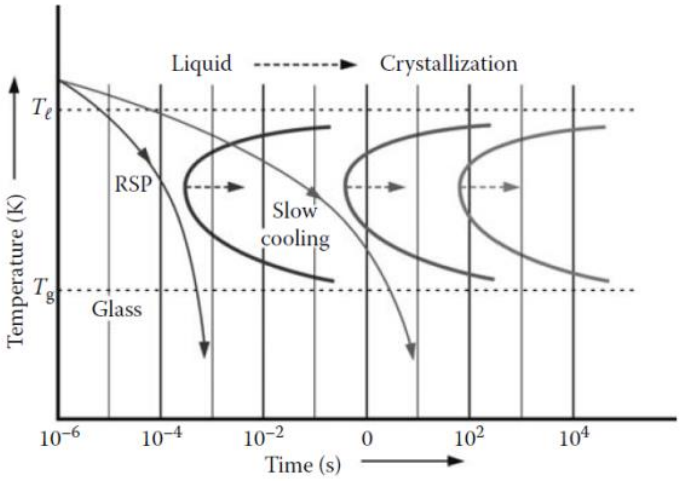

Figure 2.5:T-T-T diagram – Effect of Rapid Cooling (Suryanarayana and Inoue, 2011).

On the other hand, an entirely amorphous sample can also be obtained in case R_c is higher at the surface of the sample. It is also possible to have a thin crystalline layer formed on the surface with a glassy phase in the region due to heterogeneous nucleation at the surface irrelevantly to R_c value (Suryanarayana and Inoue, 2011).

Table 2.1: Some Representative Critical Cooling Rates (*R*c) for Formation of Glassy Phases in Different Alloy Systems (Suryanarayana and Inoue, 2011).

Alloy Composition	R(Ks^{-1})
$Au_{77.8}Ge_{13.8}Si_{8.4}$	$3 . 10^6$
$Ca_{60}Mg_{25}Ni_{15}$	24
$Ca_{65}Mg_{15}Zn_{20}$	<20
$Cu_{50}Zr_{50}$	250
$Cu_{48}Zr_{48}Al_4$	<40
$Cu_{42}Zr_{42}Ag_8Al_8$	4.4
$Fe_{43}Cr_{16}Mo_{16}C_{10}B_5P_{10}$	100
$Zr_{57}Cu_{15.4}Ni_{12.6}Al_{10}Nb_5$	10
$Zr_{65}Al_{7.5}Ni_{10}Cu_{17.5}$	1.5
$Pd_{40}Cu_{25}Ni_{15}P_{20}$	0.150
$Pd_{81}Si_{19}$	6
$Ni_{62}Nb_{38}$	57
$Ni_{65}Pd_{15}P_{20}$	105

2.4.4 Reduced glass transition temperature

It is a well-known fact that in order to obtain high glass formation a high value of T_g and a low value of T_l is required. This ratio is called reduced glass transition temperature and is denoted by T_{rg}.

$$T_{rg} = \frac{T_g}{T_l} \quad \text{(2.5)}$$

According to the nucleation theory, Turnbull suggested that at $T_{rg} \geq 2/3$, homogeneous nucleation of the crystalline phase is completely suppressed. Most typically, a minimum value of 0.4 as reduced glass transition temperature has been found to be necessary for an alloy to become a glass, but the higher the T_{rg} value, the easier it is for the glass to form (Suryanarayana and Inoue, 2011).

T_{rg} is useful in making kinetic approaches to avoid crystallization. However, T_g varies much more slowly with solute concentration than the liquidus temperature, T_l. As a result of this, the value of T_{rg} increases with increasing solute content, until the eutectic composition. Due to that, it becomes easier to avoid crystallization of the melt at the eutectic composition systems. Since the variation of viscosity with temperature show difference for different alloy systems, T_g alone may not provide information about the variation of viscosity with temperature and therefore, the T_{rg} criterion may not be valid in some systems. (Suryanarayana and Inoue, 2011)

Table 2.2: Reduced Glass Transition Temperatures (T_{rg}) for Different Glass Forming Alloys (Suryanarayana and Inoue, 2011).

Alloy Composition	T_{rg}
$Ca_{65}Al_{35}$	0.69
$Ca_{57}Mg_{19}Cu_{24}$	0.64
$Cu_{65}Hf_{35}$	0.62
$Cu_{49}Hf_{42}Al_9$	0.62
$Cu_{64}Zr_{36}$	0.64
$La_{55}Al_{25}Ni_{20}$	0.71
$La_{62}Al_{15.5}(Cu,Ni)_{22.3}$	0.58
$La_{50.2}Al_{20.5}(Cu,Ni)_{29.3}$	0.47
$Ni_{62}Nb_{38}$	0.60
$Ni_{61}Nb_{33}Zr_6$	0.49
$Pd_{40}Ni_{40}P_{20}$	0.67
$Zr_{45.38}Ti_{9.62}Cu_{8.75}Ni_{10}Be_{26.25}$	0.50

Examples for reduced glass transition temperatre for Ca-based, Cu-based, La-based , Ni-based, Pd-based, Zr-based bulk metallic glass compositions can be seen in table 2.2.

2.4.5 Deep eutectics

Apart from the systems at which liquidus temperature is observed to decrease by increasing the number of alloying elements there are alloy systems that has remarkably lower eutectic temperatures compared to the melting points of its components, which provide suitable cases for glass formation. This kind of systems are named as “deep eutectic” systems.In such cases, the T_{rg} (= T_g/T_l) value around the “deep” eutecticcomposition is a strong function of the alloy composition and exhibits thehighest value at the eutectic composition. Therefore, it should be possibleto quench this alloy composition easily into the glassy state. However, assuming that the liquidus temperature of an alloy also decreases slowly with thesolute content, then the T_{rg} value at the eutectic composition may not be high(Suryanarayana and Inoue, 2011). A number of binary phase diagrams, e.g., Au–Si, Pt–Si, and Fe–B show the variation of T_l with composition similar to that in the Pd–Si system. Therefore,an alloy with the eutectic composition, especially if it is a deep eutectic, willbe the easiest to form the glassy phase in the alloy system (Turnbull, 1974).

Due to the fact that it is not possible to obtain the phase diagrams of the multicomponent BMG alloy systems, eutectic temperatures at the binary and ternary phase diagrams of the components are studied. Even though this criterion can also be used to identify alloy compositions, same reactions tend to be observed forthe multicomponent systems in general.

Besides, DSC and DTA analyses are to be applied in order to evaluate glass formation behaviour. The composition is determined to be eutectic in case the melting takes place at a particular temperature. However, it suggests an off-eutectic point if melting takes place over a range of temperatures (Suryanarayana and Inoue, 2011).

In thermodynamic aspects, the (disordered) liquid state is preferred energetically over the solid (ordered) crystalline phases at the deep eutectic composition,either through the destabilization of the crystalline phases or through the stabilization of the liquid state. Moreover, the driving force for the nucleation and growth of the crystalline phases below the eutectic temperature (which is the energy difference between the liquid and crystalline phases) is smaller at the eutectic composition than that of the off-eutecticcompositions. Consequently, it is easier to quench the eutectic liquid intothe glassy phase without a significant crystalline phase formation. As

many crystalline ordered phases begin to compete with each other for nucleation and growth, a remarkable rearrangement of the different types of atoms is required which makes glass formation at eutectic composition favorable (Suryanarayana and Inoue, 2011).

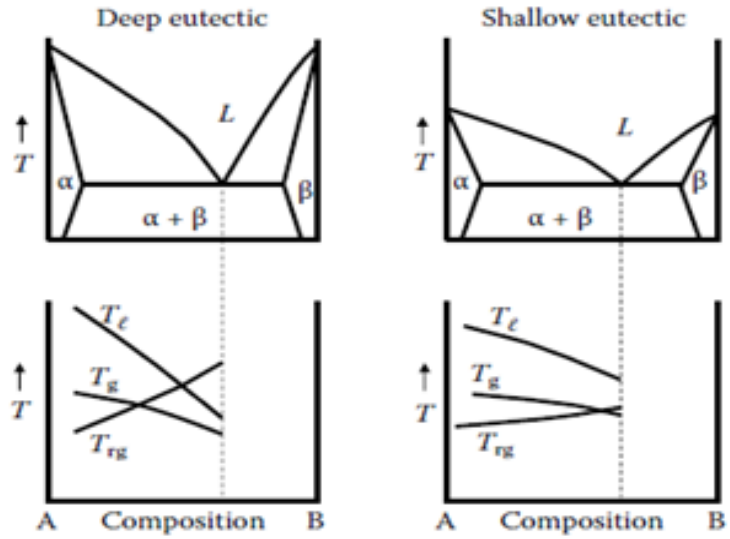

Figure 2.6: Deep eutectic and shallow eutectic formation (Suryanarayana and Inoue, 2011).

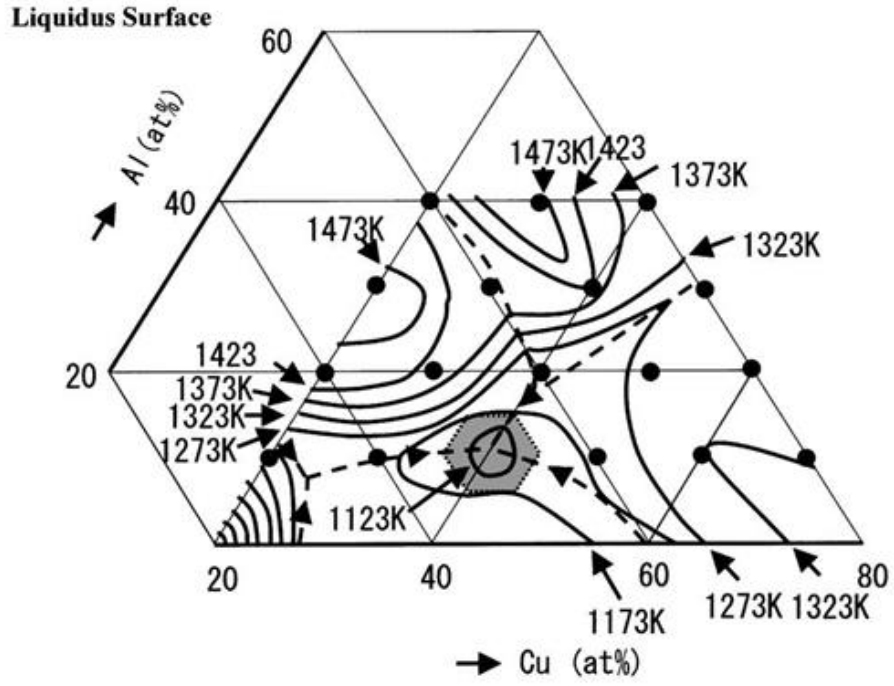

Figure 2.7: Liquidus temperature of eutectic and off-eutectic compositions at Zr-Cu-Al system (Yokoyama, Fukaura and Inoue, 2002).

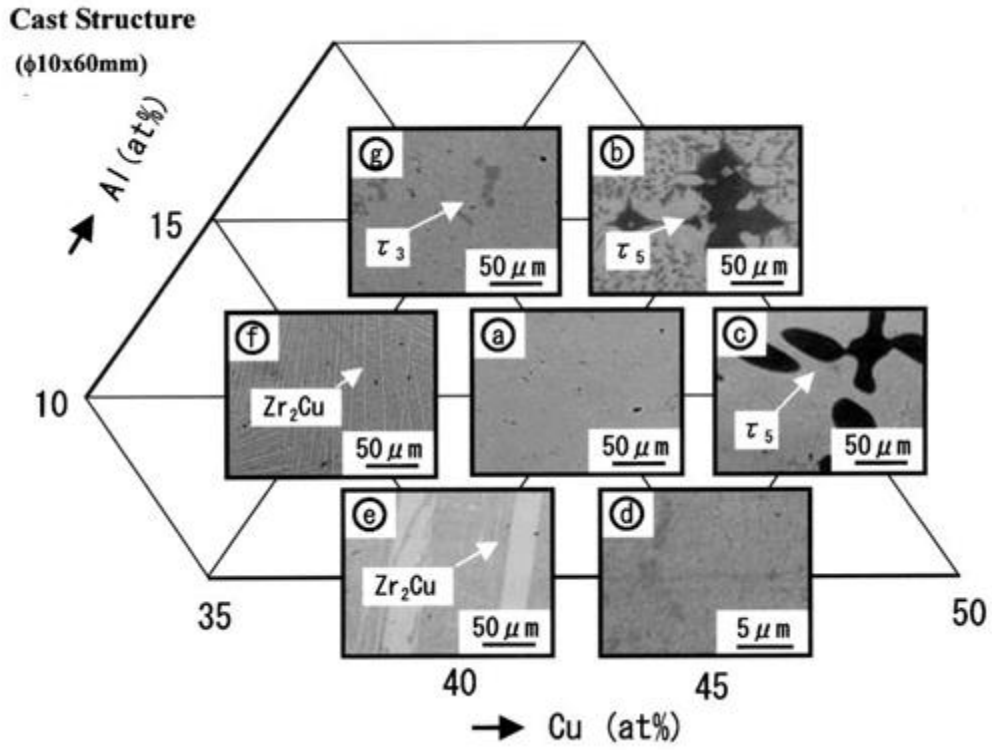

Figure 2.8: Microstructure of eutectic and off-eutectic compositions in Zr-Cu-Al system (Yokoyama, Fukaura and Inoue 2002).

The difference between the microstructures of eutectic and off-eutectic compositions can be seen in figure 2.8.

2.4.6 Role of minor alloying

Though compositional dependence of glass-forming ability (GFA) and thermal stability in various systems has been clarified, due to their limited GFA, low thermal

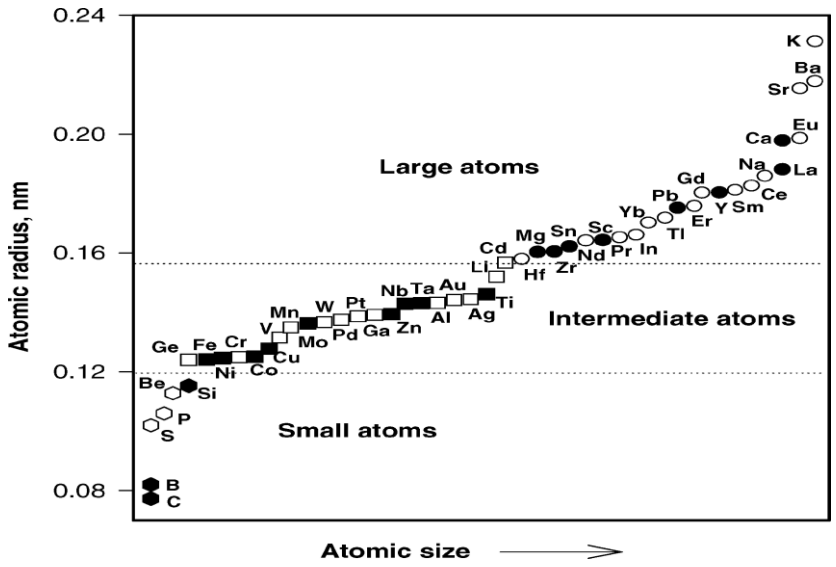

Figure 2.9: Atomic radius vs. atomic size (Lu and Liu, 2004)

stability and unsatisfactory manufacturability, their commercialization has been restricted.However, there have been a number of significant improvements that minor alloying, or microalloying, has provided in glass formation and thermal stability. Minor alloying additions have been quite useful in developing novel crystalline alloys since the last decades of 20th century. Addition of different sizes of atoms has been observed to cause different glass formation results to occur (Lu and Liu, 2004).

2.4.6.1 Addition of small atoms:

Not having oxygen completely removed from the composition is known to cause detrimental effect in glass formation, particularly in Zr-based bulk metallic glasses due to the high oxygen affinity of zirconium. It was shown that up to 2%, carbon addition was effective in improvement of glass formation (Lu and Liu, 2004).

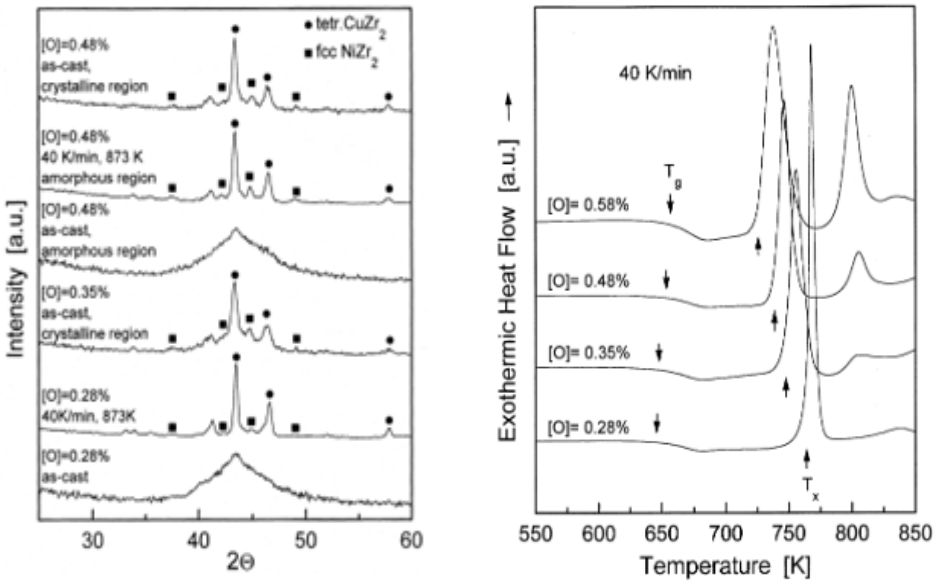

Figure 2.10: XRD patterns for bulk $Zr_{65}Al_{7.5}Cu_{17.5}Ni_{10}$ (left); DSC analysis for bulk $Zr_{65}Al_{7.5}Cu_{17.5}Ni_{10}$ (right) (Gebert, Eckert and Schultz, 1998).

Gebert et al. (1998) claimed that of more than 0,28% oxygen presence in $Zr_{65}Al_{7,5}Cu_{17,5}Ni_{10}$ metallic glass leads to crystal formation in the structure which can be seen in figure 2.8. Crystallized regioned in the cross-sectional area of $Zr_{65}Al_{7.5}Cu_{17.9}Ni_{10}$ bulk metallic glass composition can be discerned in the micrograph having released the amorphous matrix featureless.

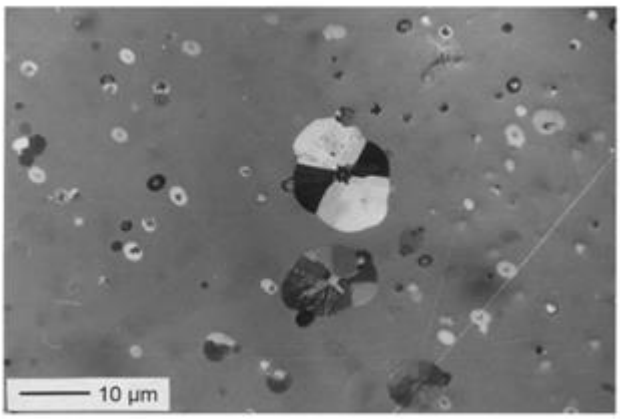

Figure 2.11: Light microscopy image of the cross-sectional area of a bulk $Zr_{65}Al_{7.5}Cu_{17.9}Ni_{10}$ (Gebert, Eckert and Schultz, 1998).

Regarding the research carried out by Kündig et al (2002) there was a reverse proportion among the oxygen concentration and maximum $Zr_{52,5}Cu_{17,9}Ni_{14,6}Ti_5Al_{10}$ (Vit105) thickness obtained by casting.

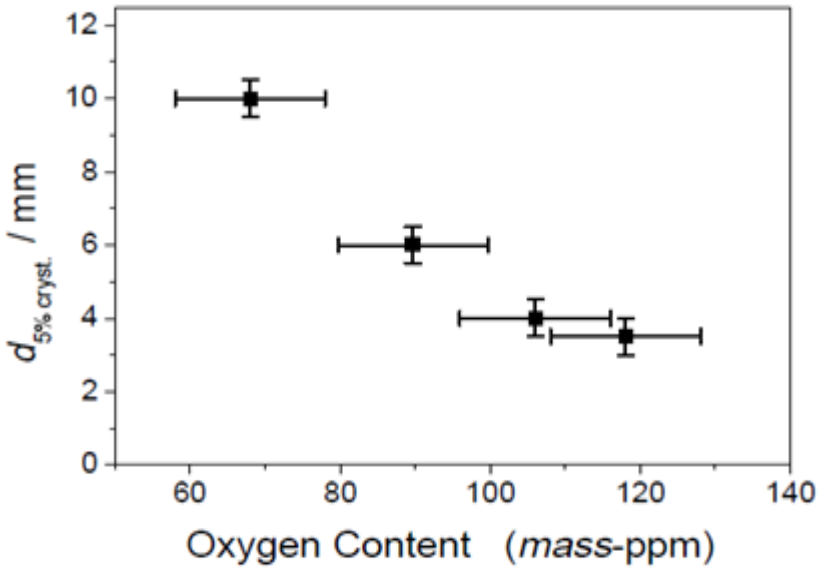

Figure 2.12: Glass forming ability of $Zr_{52.5}Cu_{17.9}Ni_{14.6}Al_{10}Ti_5$ in function of residual oxygen contents. The glass forming ability is given as amorphous phase in castingsinto copper mold. (Kündig, 2002).

Silicon is effective in facilitating glass formation for refractory-elements-based alloys such as Cu-, Fe- and Ni-alloys. In alloy $Cu_{47}Ti_{34}Zr_{11}Ni_8$, substituting only 1% Ti with Si, increased its maximum diameter for glass formation from 4 to 7 mm (Choi-yim, Busch and Johnson,1998). However, it is very interesting to point out that Si additions of even 1 at.% are extremely detrimental to the GFAof Zr-based alloys due to the formation of silicides (Lu and Liu, 2004). Kündig et al. (2002) asserted

that For Si additions; no significant decrease in oxygen content dissolved was investigated in $Zr_{52.5}Cu_{17.9}Ni_{14.6}Ti_5Al_{10}$ due to the increased content dissolved within the composition. Also, a decrease in GFA was observed due to its addition.

Table 2.1 : Nominal, prepared and measured carbon concntrations as well as measured oxygen contents and values for mass loss during melting in the carbon alloyed samples (Lu and Liu, 2004)

Nominal carbon [at%]	Prepared carbon[at%]	Measured carbon[at%]	Metallography 5% crystallography [mm]	Oxygen content [mass-ppm]	Mass loss melting [%]
0.1	0.097	0.103	5.7	96	0.11
0.3	0.297	0.204	3.8	92	0.10
1.0	0.992	0.790	4.2	132	0.18

For C additions; addition up to 0.1% enhanced GFA in Vit105. Increasing the amount of it hinders its dissolution. At 1% C addition, slag layer formed over the melts. Higher values of addition brings the risk carbide formations (Kündig et al, 2002).

Despite the fact that addition of boron might result in boride formation, an optimum addition of boron along with Si and Pb with a ratio of 0.1 at B+ 0.2 at. Si+ 0.1 at Pb provided full amorphous structure for Vit 105 (Liu, Chisholm and Miller, 2002).

Depending on their limited solubility in the competing crystalline phases, extra small atoms show a long-range redistribution during the crystallization process upon undercooling. Consequently, a high concentration layer of these atoms ahead of the solid/liquid interface is built up which hinders the nucleation and growth processes (Lu and Liu, 2004).

Small atoms tend to occupy interstitial spaces among the major constituent atoms that results in an increase in the packing density of the liquids. Meantime, due to the strong atomic bonding between metalloids and metallic elements, additions of small metalloid atoms can enhance the short-range compositional order of glass-forming liquids. As such, the liquid phase stability is improved. These small metalloid atoms can also suppress the formation of the competing crystalline phases in off-eutectic compositions and adjust the composition close to the eutectic. As a result of this, a decrease occurs in the melting point of the resulting alloy is observed (Lu and Liu, 2004).

2.4.6.2 Additions of intermediate atoms

Transitional metals with intermediate atomic sizes,such as Fe, Ni, Co, Cu, Mo, Zn, Nb,Ta andTi, have been selected as minor alloying elements in various systems. Surprisingly, most of them are detrimental to glass formation (Lu and Liu, 2004). Only when their alloying quantitiesexceed 3 at.% and become a major constituent of the system, have they been shown to be beneficial in bulk glass formation. For example, in order to improve the GFA of alloy $Mg_{65}Cu_{25}Y_{10}$, the addition of Zn has to be at least 5 at.% (Men, Hu, and Xu, 2002).

For Ca additions; mass losses were observed due to slag layer and large quantities of dust formations. A decrease in GFA was observed due to the increasing amount of its addition (Kündig, 2002).

Using metals with intermediate atomic sizes seemed to be less effective on glass formation. In general, regarding the Hume-Rothery rules, they form solid solutions with other constituents during solidification. For example, in alloy $Nd_{60}Fe_{20}Al_{10}Co_{10}$, for example, replacing 2.5% Nd with Cu actually degraded its GFA. This degradation can be ascribed to: (1) the marginal mismatches of atomic sizes between Fe, Al, Co and Cu, and (2) the high tendency of forming solid solutions between Fe, or Co and Cu (Lu and Liu, 2004).

2.4.6.3 Additions of large atoms

Large atoms, such as Zr, Sn, Sc,Yand Pb, are helpful in terms of glass formation (Lu and Liu, 2004). Microalloying with 2 at.% Y in Zr- and Fe-based alloys greatly enlarged their attainable maximum sizes for these alloys even with low-purity rawmaterials.

A similar beneficial effect of Sc was observed in a Zr-based alloy (Kundig, 2002). With additions of 300 to 600 ppm Sc, the maximum diameter for glass formation of alloy $Zr_{52.5}Al_{10}Ti_5Cu_{17.9}Ni_{14.6}$ containing 90–120 wppm oxygen was increased from 4.5 to 12mm (Kündig, 2002). The addition of Sc created beneficial results in cases at which low purity raw materials were used (Jang, Wang, Zhang and Sun, 2005). As a 3B group metal Sc is a metal that tends to dissolve oxygen. The fact that Sc has a higher oxygen affinity than Zr also contributes to that hypothesis such as it does in the cases of yttrium microalloying.

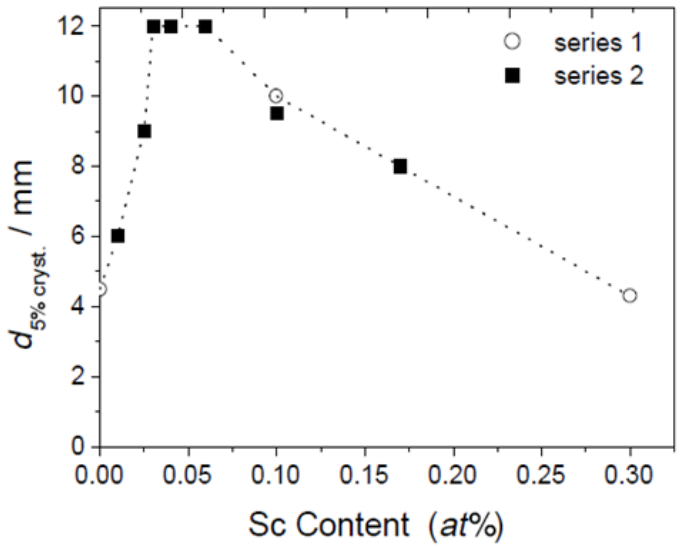

Figure 2.13: Influence of Sc additions in $[Zr_{52.5}Cu_{17.9}Ni_{14.6}Al_{10}Ti_5]_{100-x}Sc_x$ (Kündig, 2002).

For La additions;GFA was observed to be increasing by the increasing content of La. However, complete dissolution could not be achievieved for additions higher than 3% (Kündig , 2002).

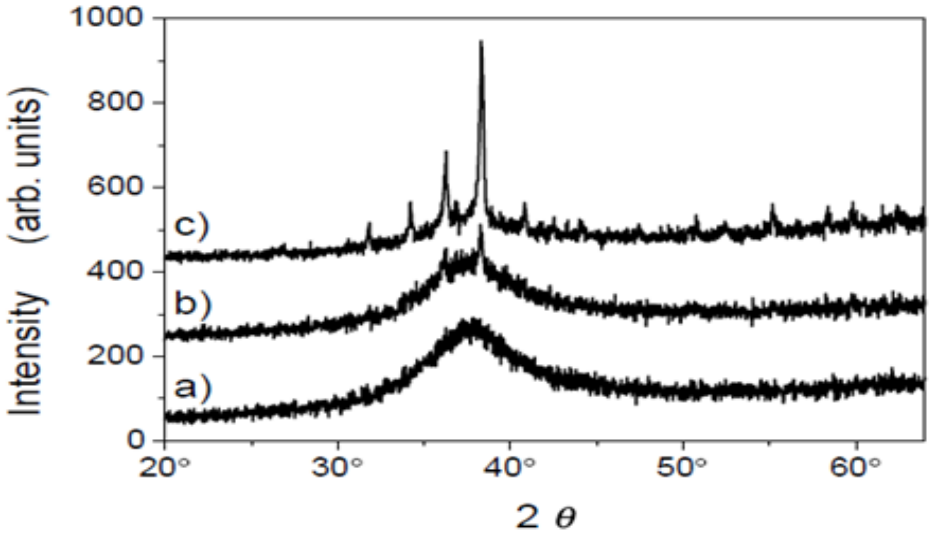

Figure 2.14: Sequence of X-ray diffraction patterns with increasing crystalline phase content on cuts of the original alloy $Zr_{52.5}Cu_{17.9}Ni_{14.6}Al_{10}Ti_5$ (Kündig , 2002).

Also, yttrium was found to be able to not only scavenge oxygen from the undercooled liquid but also lower the liquidus temperature in some Fe-based alloys (Lu, Liu and Porter, 2003). Tin is extremely effective in promoting glass formation for refractory-elements-based alloys (Lu and Liu, 2004). Replacing only 2 at.% of Ni

with Sn in alloy $Cu_{47}Ti_{33}Zr_{11}Ni_8Si_{10}$, for example, increased its maximum size for glass formation by 2 mm (Park, Lim, Kim, and Kim, 2002). It is to be noticed that some large elements like La, Ca, Sb, etc., have negative effects on the GFA of some Zr- and Ti- based BMGs (Lu and Liu, 2004).

The added large atoms have to be redistributed during the crystallization process upon cooling because of their limited solubility. Primarily, the additions of these atoms make it difficult for the concentrations of all elements to simultaneously satisfy the composition requirements of the crystalline nucleus because of having long-range rearrangement of more kinds of atoms involved. Furthermore, rejecting these large atoms from the crystalline nucleus changes the composition and interfacial energy at the solid/liquid interface. Additionally, essential long-range inter-diffusions decrease the rate of the subsequent crystal growth rate of the nucleus. These factors suppress the formation and growth of the competing crystalline phases. Consequently, enhancement in glass formation is observed (Lu and Liu, 2004).

In terms of thermal stability following factsare noteworthy: Firstly, depending on their low solubility in the competing crystalline phases, involving these large atoms in off-eutectic alloys tend to effectively suppress the formation of the competing crystalline phases (i.e., primary phases in these cases) and conform the composition close to the eutectic. Consequently, the melting point is decreasedand the liquid phase is stabilized. Secondly, as large elements generally have a high tendency of compound formation with major constituents in a base alloy which increases its short-range compositional ordering and favors the formation of clusters in the undercooled liquid. Experimental studies have revealed that the local chemical configuration of the clusters in undercooled liquids showed significant differences compared to that of the long-range crystalline ordering In order to form crystalline structure, the atomic pairs in these clusters have to be broken apart upon cooling to form new, stronger chemical bonds with the other constituents. (Lu and Liu, 2004).

It was found out that microalloying with Y in several Cu- and Fe-based alloys can greatly improve their GFA via lowering their liquidus temperatures (Lu and Liu, 2004). Besides for Vit105, it was revealed that microalloying with Y was quite effective in enhancement of glass formation in case the ratio of it is optimized (Peng, and Zang, 2010).

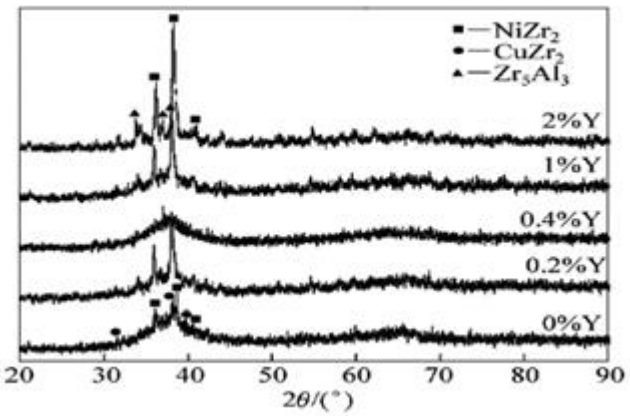

Figure 2.15: XRD patterns of (ZAT)100-xYx (x=0,0.2,0.4,1,2) (Peng and Zhang, 2004).

2.4.6.4 Addition of crystallization anticatalysts

Depending on the fact that it is a very challenging process to avoid the detrimental effects of oxygen impurity in BMGs such as Zr- and Fe-based alloys, minor alloying technology has a special importance.For instance, Liu *et al*. (2002) asserted that adding 0.1% B, 0.2% Si and 0.1% Pb to $Zr_{52.5}Al_{10}Ti_5Cu_{17.9}Ni_{14.6}$ alloy that contained about 3000 appm oxygen.

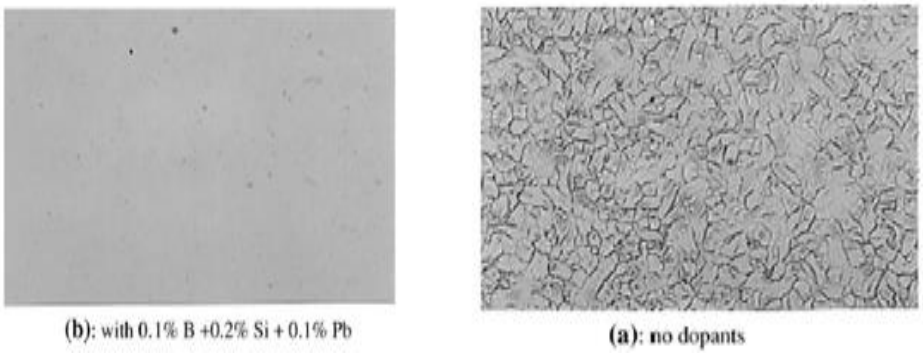

Figure 2.16 : Micrographs of as-cast 6.4 mm rods of alloy $Zr_{52.5}$ $Al_{10}Ti_5Cu_{17.9}Ni_{14.6}$ with (a) and without (b)dopants of 0.1%B + 0.25%S0.1 %Pb (Kündig, 2002).

provided a successful microstructure.It can be seen in the figure that presence of dopants made the structure of the alloy fully amorphous.

In Zr-based alloys formation of tiny Zr_4Ni_2O particles is inevitable; however, as can be seen from figure 2.16, microalloying prevents the growth of these particles, and frees the amorphous structure from oxygen presence, therefore leaves the amorphous matrix stabilized.The reasons lying behind this mechanism might be either the the change in the interfacial structures and chemical composition which suppresses crystal formation, or stabilization of the glass matrix, that is freed from oxygen,

which prevents the crystallization to be triggered. Similar results in other Zr-based alloys were reported using Sc, Y, C, etc., as crystallization anticatalysts (Lu and Liu, 2004).

It was also revealed that Y could effectively neutralize oxygen in the undercooled liquid of Fe-based alloys (Lu, Liu and Porter, 2003).As such, the GFA of these alloys was greatly improved. Back-scattered electron microprobe micrographs for the central part of 5 mm drop-cast samples for alloys (a) $Fe_{63}Zr_8Co_6Al_{11}Mo_7B_{15}$ and (b) $Fe_{61}Y_2Zr_8Co_6Al_{11}Mo_7B_{15}$ are shown in figure 5. Without the addition of yttrium (Figure 5a), alloy $Fe_{63}Zr_8Co_6Al_{11}Mo_7B_{15}$ shows typical dendrite phases (dark phase) embedded in the amorphous matrix. For the alloys containing yttrium, only a few spherical particles embedded in the amorphous matrix were seen, as shown in figure 5b. These observations obviously demonstrated the beneficial effect of yttriumaddition on glass formation. The dark particles in figure 5b were identified as yttrium oxides.

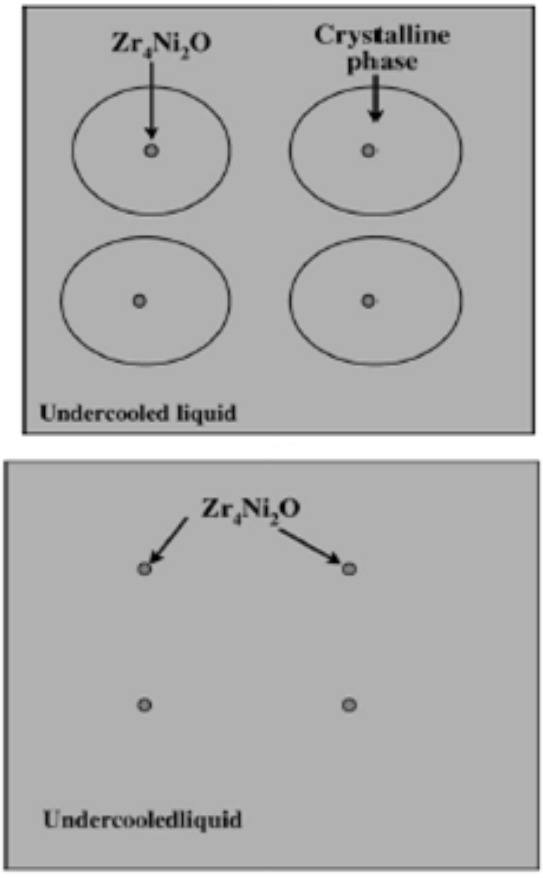

Figure 2.17: Sketch to show the beneficial effect of the optimum dopants (left) no dopants and (right)with optimum dopants (Lu and Liu, 2004).

Thermodynamically, yttrium has a stronger affinity for the oxygen atom compared with the other elements in the system. The heat of formation of yttrium oxide is 1903.6 KJ/mol, the highest among all oxides of constituent elements (Fe_2O_3, 820.5 kJ/mol; ZrO, 1102.3 kJ/mol; MoO_3,744.5 kJ/mol; Cr_2O_3, 1128.6 kJ/mol) (Kubaschewski and Alcock, 1979). The reaction between Y and O is thermodynamically favored compared to the reaction between O and the other elementsin the system. In the molten liquid, yttrium becomes partially neutralized with the oxygen during the melting and casting processes.The content of oxygen in the remaining liquid was much decreased as yttrium acts as a scavenger. Besides, because of their crystallographic structures sizes (too small or too large to be the crystallization catalyst), dispersion and wetting behavior between solid/liquid interfaces, the yttrium oxides did not tend to behave as heterogeneous nucleation sites, remaining the liquid fully amorphous upon continuous cooling.

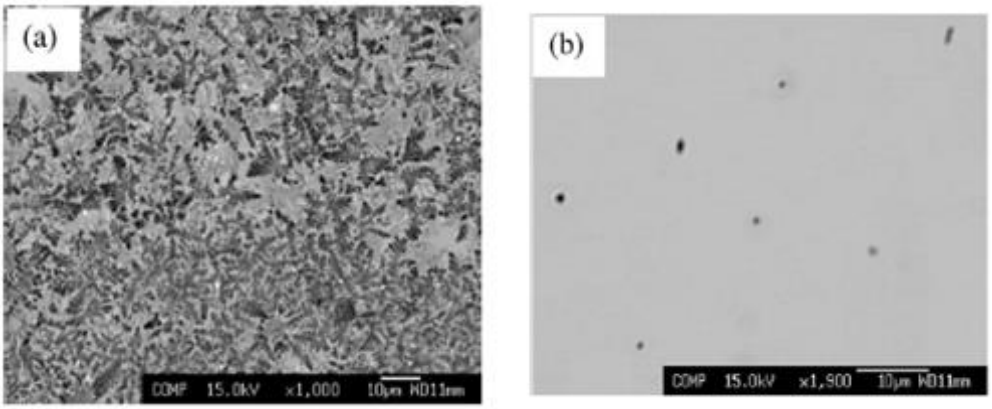

Figure 2.18: Back scattered electron microprobe micrographs for the central part of 5 mm dropcast samples for alloys (a) $Fe_{63}Zr_8Co_6Al_1Mo_7B_{15}$ (b)$Fe_{61}Y_2Zr_8Co_6A_{l1}Mo_7B_{15}$ (Lu and Liu, 2004).

Therefore, from a microalloying technological point of view, the GFA of glass-forming liquids can be enhanced by the following considerations:

(a) choose additional elements having large atomic mismatches with the major constituents;

(b) select elements having high tendency of compound formation (e.g., negative heat of mixing); and

(c) minimize oxygen impurity via microalloying with certain elements (Lu and Liu, 2004).

2.5 Synthesis Methods of Bulk Metallic Glasses

Metallic glasses have been produced by rapidly solidifying metallic melts at cooling rates of about 106 K s−1. This early excitement of being able to produce the normally crystalline metals in a glassy state, and their excellent mechanical, chemical, and magnetic properties, led to the development of a variety of techniques to obtain metallic glasses in different sizes and shapes (ribbons, wires, powders, etc.). The commercial requirements of large-size sheets for different applications resulted in the development of the planar flow casting method, wherein rapidly solidified sheets of at least 30 cm in width could be produced. The quest for bulk glassy alloys for industrial applications eventually culminated in the discovery of bulk metallic glasses (BMGs). BMGs have been produced at relatively slow solidification rates of about 103 K s^{-1} or less. But, before describing the different techniques to synthesize BMGs, let us briefly look at the requirements for rapid solidification processing (RSP) and the important techniques used to produce rapidly solidified ribbons. This assumes relevance here because a lot of researchers in the field of BMGs still use the melt-spinning technique to produce ribbons and study their properties and crystallization behavior before proceeding to investigate the synthesis and characterization of BMGs.

2.5.1 Melt spinning

In the melt-spinning method, a small quantity of the alloy is melted inside a crucible or by levitation methods, and then ejected by pressurization through a fine nozzle onto a fast-rotating copper wheel. Every one of these parameters can be carefully controlled to obtain the desired size, shape, and thickness of the ribbon (Suryanarayana and Inoue, 2011).

Wheels for melt spinning have been made from a variety of materials, including copper, stainless steel, chromium, and molybdenum, although copper is the most popular one. The primary purpose of the wheel is to extractthe heat from the ribbon as quickly as possible, while allowing the puddle to wet the wheel and form the ribbon. Cooling of the wheel is desirable for long runs. The outer surface of the wheel is generally polished to remove any surface roughness since the wheel side of the cast ribbon is almost an exact replica of the wheel surface (Suryanarayana and Inoue, 2011).

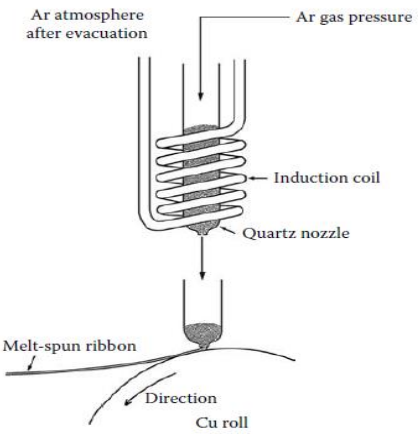

Figure 2.19: Melt spinning (Suryanarayana and Inoue, 2011).

2.5.2 Flux melting technique

The work of Drehman et al. (1982) clearly showed that removal of heterogeneous nucleation sites is very important in suppressing the nucleation of crystalline phases. Another way by which the impurities present in the alloy could be removed is to heat and cool the molten metal while it is immersed in a molten oxide flux. After gravity segregation, the impurities present in the alloy get dissolved in the molten oxide flux. If the flux (like the slag in foundries) containing the impurities from the alloy is maintained in the liquid state at the glass transition temperature of the alloy, *T*g, that is, when the glass is formed, then glass formation can be achieved at slower solidification rates. And, slow solidification rates translate to large section thicknesses. Using this logic, Kui et al. (1984) produced a 10 mm size glass in 1984. They used anhydrous boron oxide (B_2O_3) to remove the impurities from the $Pd_{40}Ni_{40}P_{20}$ alloy melt. At the glass transition temperature of $Pd_{40}Ni_{40}P_{20}$ (~600 K), B_2O_3 was still in the molten state. Thus, by heating this alloy to higher temperatures (~1273 K) and cooling it slowly to temperatures below *T*g of the alloy, these investigators were able to produce 10 mm size glassy samples of $Pd_{40}Ni_{40}P_{20}$ using this technique. Incidentally, this was the first time that the term "bulk metallic glass" was used in the title of the publication. This method has now come to be known as the fluxing or flux-melting technique and continues to be popular to remove impurities from the melt and to avoid heterogeneous nucleation events.

2.6 Casting Bulk Metallic Glasses

2.6.1 Water quenching method

The quenching medium (water) extracts the heat rapidly from the hot steel specimen and as a result the austenite phase transforms to the martensitic condition in a diffusionless manner. The cooling rates achieved by the water quenching method are inherently dependent on the heat transfer efficiency of the quenching medium, the size of the steel specimen, and its heat transfer properties. The cooling rates achieved by this method have been usually reported to be about 10–100 K s^{-1}. Since some of the BMG alloy compositions require very low critical coolingrates for glass formation, it is possible to produce glasses in these alloys by this simple technique of water quenching. Inoue et al. (1989) produced 1.2 mm diameter $La_{55}Al_{25}Ni_{20}$ glassy rods by quenching the melt contained in a quartz capillary into water.

2.6.2 High pressure die casting

Figure 2.19 shows the schematic of the high-pressure die-casting equipmentdesigned and used by Inoue et al. (1992) to synthesize Mg-based BMGs. The main components of the equipment are a sleeve to melt the alloy, a plunger topush the molten alloy through hydraulic pressure into the copper mold, and a copper mold to solidify the melt. The whole unit is evacuated to prevent gas entrapment by the melt and consequent porosity in the casting.

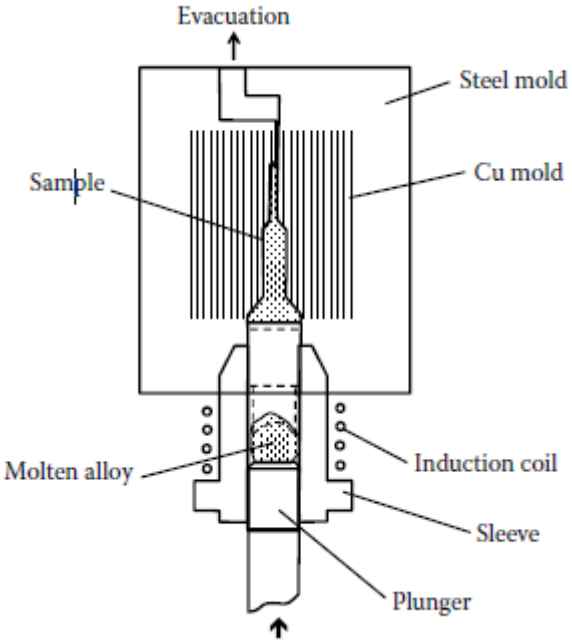

Figure 2.20: High Pressure Die Casting (Suryanarayana and Inoue, 2011).

Most frequently, the alloys are melted by induction-melting techniques, but sometimes they are prepared by arc melting the pure metals under a Ti-gettered argon atmosphere in a water-cooled copper crucible. The molten alloys are melted repeatedly several times to ensure compositional homogeneity. When melting of alloys with a high vapor pressure, for example, magnesium (or other materials), is carried out, about 5 wt.% of excess amount of magnesium is added to compensate for the loss of magnesium through evaporation during repeated melting operations. The molten alloy is then poured into a copper mold.

2.6.3 Copper mold casting

Generally, a low pressure (0.05 MPa = 50 kPa) is applied to eject the metal from the crucible toward the mold. The temperature of the molten metal can be maintained in such a way that it continues to be in the liquid state during the whole process of ejection until it fills the mold cavity. The casting can be done in air or vacuum, inert atmosphere, or under argon, if oxidation has to be avoided.

Inoue et al. (1995) placed platinum – rhodium (Pt-Rh) thermocouples at different positions along the length of the wedge-shaped mold to measure the cooling rates and eventually determine the continuous cooling transformation (CCT) diagrams.

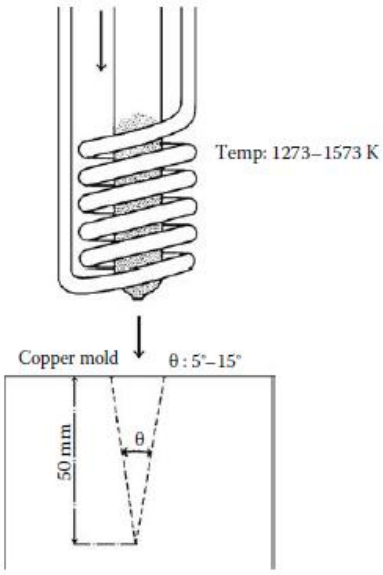

Figure 2.21: Copper Mold Casting (Suryanarayana and Inoue, 2011).

Samples could be collected from different positions in the mold for characterization by x-ray diffraction, optical microscopy, transmission electron microscopy, and DSC

to determine the true glassy nature of the cast material and also to study its transformation behavior to the equilibrium crystalline state.

2.6.4 Cap-cast technique

The biggest advantage of this technique is that high cooling rates are achieved not only on the sides and bottom of the casting since they are in contact with the metal mold, but even in the upper part of the cast specimen since this is in contact with the metal cap. Using this method, the authors were able to produce a fully glassy rod of 30 mm diameter in the $Zr_{55}Cu_{30}Ni_5Al_{10}$ alloy.

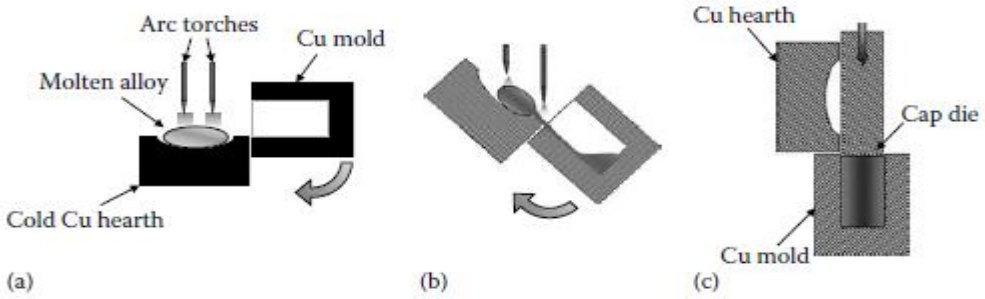

Figure 2.22: Schematic diagrams comparing the (a) arc melting, (b) tilt casting (c) cap-cast techniques used to produce bulk metallic glassy alloys (Suryanarayana and Inoue, 2011).

2.6.5 Suction casting method

The suction-casting system consists of two chambers—an upper chamber in which the alloy is melted and a lower chamber in which the casting is done in a copper mold . The two chambers are connected through an orifice, the size of which is about 2 mm to 16 mm in diameter (Gu, Xing and Hufnagel, 2002). The base of the mold is connected to a vacuum source that, when released, causes a pressure differential, which forces themelt into the chamber. When the piston separating the melting chamber and the casting chamber is removed, the differential pressure between these two chambers allows the molten metal to be sucked into the casting chamber,and then to be solidified in the copper mold.

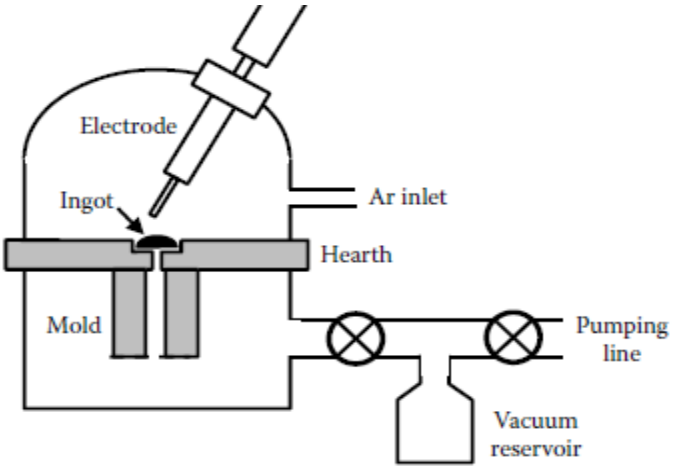

Figure 2.23: Schematic diagram of the arc melting/suction casting apparatus (Suryanarayana and Inoue, 2011).

2.6.6 Squeeze casting method

Sometimes the cast BMG alloys have some porosity in them. Further, it would be also desirable to have net-shape forming capability during the casting process. Squeeze casting has a high potential to achieve such features. The squeeze-casting process involves solidification of the molten metal under a high pressure within a closed die by utilizing a hydraulic press (Lynch, Olley and Gallagher, 1975).

2.6.7 Arc melting method

This is a method that can be used to obtain glassy phases in alloy systems that require a low critical cooling rate for glass formation. The procedure used here is to arc melt the alloy on a copper hearth. Once the alloy is molten, the copper hearth acts like a heat sink and extracts the heat from the melt. This is somewhat similar to the method of producing rapidly solidified alloys by laser processing, wherein the heat from the molten alloy is rapidly extracted by the large solid mass with which the molten pool is in contact. Optical micrographs of arc-melt cast samples show the presence of chill zone and columnar zone very clearly at the edges of the casting and the glassy phase in the center of the casting (Inoue, 1998).

2.6.8 Unidirectional zone melting method

In this method, a small region of a long and impure metal bar is melted, and this molten zone traverses alongthe length of the metal rod slowly. Because of solute partitioning effects, the solute concentration is (usually) higher in the liquid phase than in the solid phase.

Accordingly, the impurities present in the metal get segregated to the liquid phase. As the molten zone travels slowly, more and more of the impurities get segregated into the neighboring liquid phase, leaving behind a purer solid phase. If this process is repeated a few times, one ends up with an extremely pure metal rod, with all the impurities segregated to one end of the rod.

This method was originally employed to purify silicon and germanium crystals for application in transistors, but can be used for any material that needs to be purified. This technique has been successfully adopted to produce continuous BMG samples in a Zr-based alloy by Inoue and Yokoyama (1994).

2.6.9 Electromagnetic vibration process

Though the role of electromagnetism had been heavily ignored for a considerable duration, Tamura et al. (2005) showed that the application of electromagnetic vibrations induced by the interaction of alternating electric and stationary magnetic fields could act as powerful vibrating forces in the melt and affect the presence of

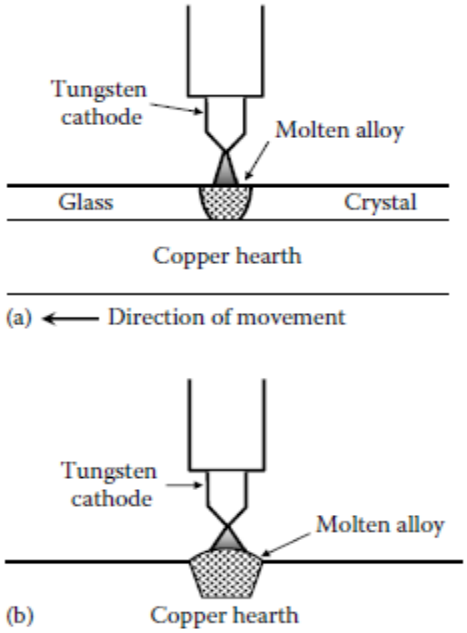

Figure 2.24: Schematic diagram of the zone-melting equipment used to produce bulk metallic glass ingot o a Zr-based alloy. a) Front view b) Side view (Suryanarayana and Inoue, 2011).

clusters that could act as nucleation sites for the formation of crystalline phases. By eliminating such clusters in the liquid state, they had demonstrated that the GFA of alloys could be substantiallyincreased.

2.7 Properties of Bulk Metallic Glasses

2.7.1 Magnetic properties

Magnetic glasses are very easy to magnetize and remagnetize because the domain walls canmove easily in the absence of lattice faults. They have

– high saturation magnetization;
– low coercivity;
– low Curie points;
– very low heat losses at magnetization and remagnetization (Fredriksson and Akerlind, 2012).

The first Fe-based BMG alloy (in the form of melt-spun ribbons) was prepared in 1995 in the $Fe_{72}Al_5Ga_2P_{11}C_6B_4$ system. This alloy had a wide supercooled liquid region of 61 K. Many other Fe-based BMGs were subsequently synthesized both by researchers in Inoue's group and others. The magnetic properties of BMGs have been investigated mostly in Fe-based BMGs, and investigations on Co-based BMGs have been carried out. The hard magnetic properties of Nd- and Pr-based alloys have also been studied (Suryanarayana and Inoue, 2011).

2.7.2 Mechanical properties

Excellent mechanical properties, reaching 10 times higher elastic strain than metals and greater fracture strength are observed for bulk metallic glasses (Fredriksson, and Akerlind, 2012).

The deformation behavior of metallic glasses is examined as inhomogeneous at low temperatures and high stresses and strain rates, and as homogeneous at high temperatures and high strain rates. At low temperatures, lower than about 0.5 *T*g, where T_g is the glass transition temperature, deformation is mostly concentrated in a few very thin "shear bands" that form approximately on the planes of maximum resolved shear stress. These planes are inclined close to 45° to the loading axis. This localized deformation is referred to as "inhomogeneous" deformation. It is the inhomogeneous deformation in the metallic glass that renders it mechanically unstable at high stresses. Consequently, it fails catastrophically (Suryanarayana and Inoue, 2011).

On the other hand, at high temperatures, greater than about 0.5 T_g, metallic glasses undergo viscous flow in which plastic strain is distributed continuously, but not

necessarily equally, between different volume elements within the material. That is, each volume element of the specimen contributes to the strain. This type of deformation is referred to as “homogeneous” deformation (Suryanarayana and Inoue, 2011).

2.7.3 Chemical properties

Bulk metallic glasses have nearly 10 times stronger corrosion resistance properties than metals (Fredriksson, and Akerlind, 2012). The corrosion behavior of BMGs becomes important when these materials need to be used in aggressive and hostile environments (high temperatures, oxidizing atmospheres, and corrosive media). Knowledge of the corrosion behavior becomes crucial when these BMGs are considered for biomedical applications and for decorative applications, or when surface appearance assumes importance (Suryanarayana and Inoue, 2011).

3. EXPERIMENTAL STUDIES

3.1 Theoretical Studies

Having all the components molten for alloy systems is a factor that eases glass formation. In $Zr_{52.5}Cu_{17.9}Ti_5Ni_{14.6}Al_{10}$ alloy, it is seen that the whole system is completely liquefied as soon as the system reaches 785.9 ^oC according to thermodynamic calculations carried out by FactSAGE 6.4.

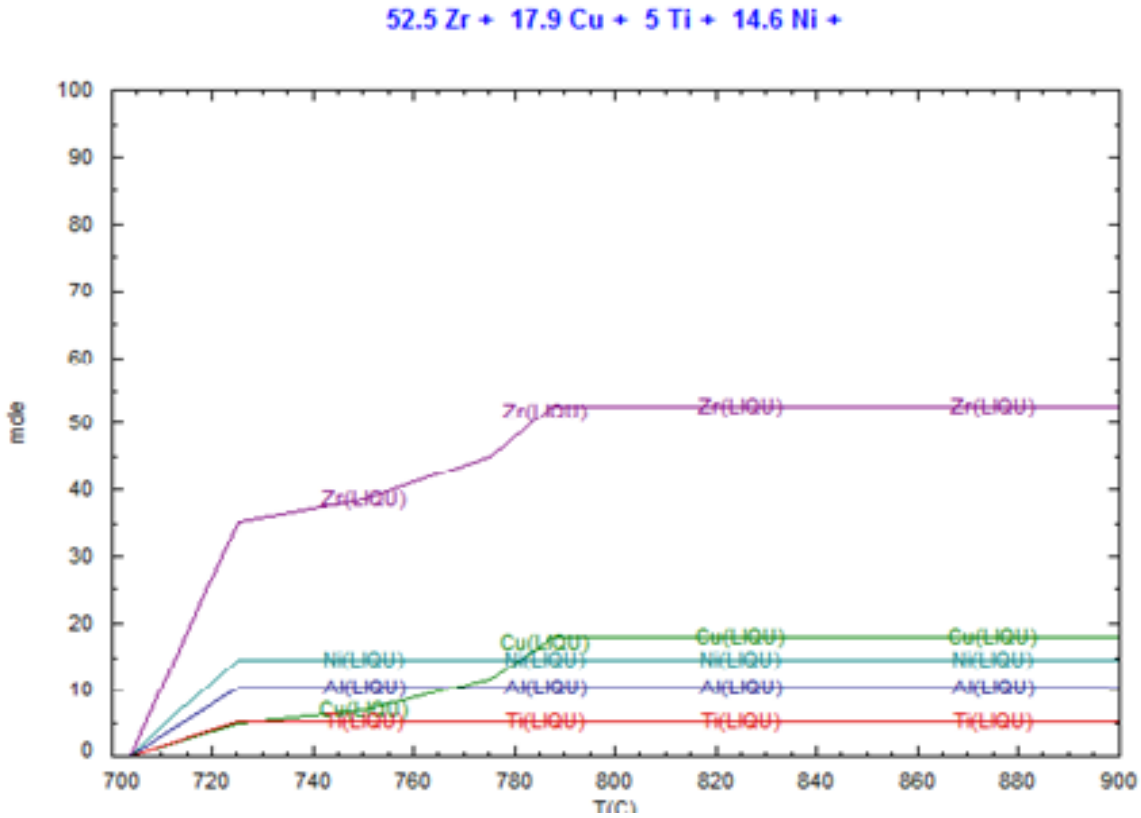

Figure 3.1: Melting behaviour of the components in the system (FactSAGE 6.4)

As a 4B group metal, zirconium has a high oxygen affinity. Having oxygen involved as an impurity makes it more difficult in bulk metallic glasses for heat to be extracted from the melt without suppression of crystallization. Regarding what was mentioned in chapter 2.4.6.3, once phases such as Zr_4Ni_2O which trigger heterogeneous nucleation forms, the structure gains the tendency to become fully crystallized. In

order to avoid this situation, microalloying with metals that have higher oxygen affinity are applied. As can be seen from the Ellingham in the figure, both hafnium and yttrium , which are also 4B group metals, have higher oxygen affinity. Among these Hf has almost the same atomic size with zirconium where yttrium is larger than it. Substitution of pure Zr with Zr that has Hf involved was assumed to have a higher entropy which enhances glass formation, on the other hand, the system has a rather high oxygen affinity which tends to cause crystallization. In order to hinder crystallization yttrium, which is an atom that reacts with oxygen to form Y_2O_3 with the oxygen in the system without causing heterogeneous crystallization, is addedto the alloy by minor alloying.

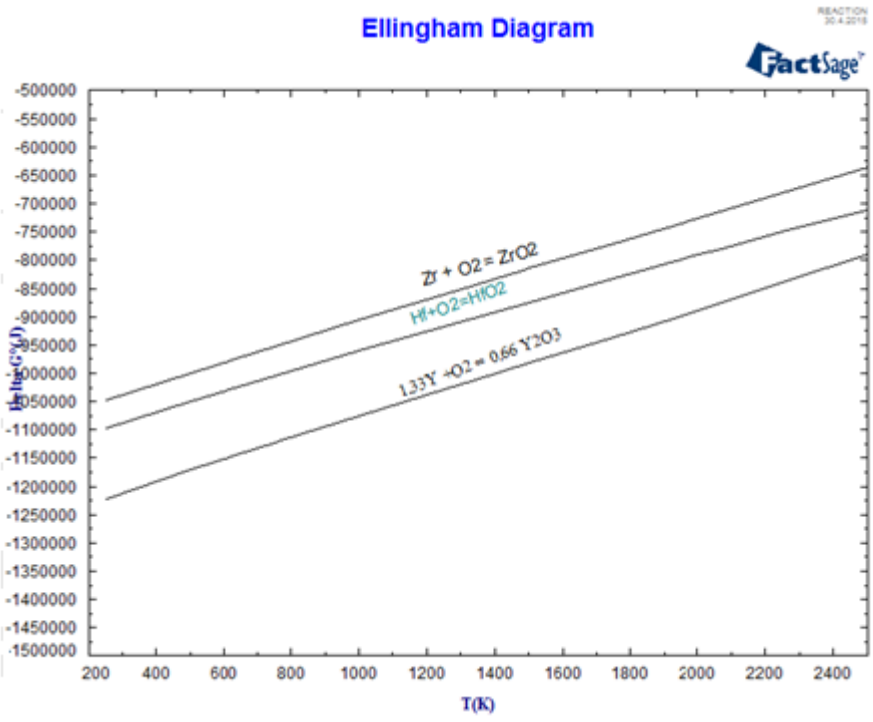

Figure 3.2: Elligham Diagram for Zr-Hf-Y (FactSAGE 6.4)

3.2 The Equipments

3.2.1 Edmund Buehler mini arc melting and suction casting equipment

In order to carry out the sample preparation studies, Edmund Buehler MAM-1 arc melter and suction casting equipment at M101 Pyrometallurgy Laboratory in I.T.U. Faculty of Chemical and Metallurgical Engineering were used. The electrode used for making arc and melting samples is tungsten. Arc with a maximum value of 200 A can be obtained. The equipment has two different copper crucibles with have pipes

delivering water mantled inside them for melting one being used as only for arc melting, the other being used for both arc melting and suction casting practices .

Figure 3.3: Edmund Buehler Mini Arc Melter

The primary one is capable of melting samples of 5-20 grams where as the latter one is used for producing cylinders in 3mm in diameter and 6 mm in length. The equipment possesses a vacuum pumping system. Gas purging and vacuum valves and manometer are attached to the system. The system shuts down in case of excessive increase in temperature and having eye protectione cover opened. Electricity source: 400 V, 3 phase / 50/60 Hz. or 230 V, 1-phase 50/60 Hz

3.2.2 Edmund Buehler arc melting equipment

The arc melting equipment in BOREN was used for sample prepation which has a copper crucible with water pipes in it. It has a capacity of melting approximately 200 g of samples. The values of electricity current applied and the evacuation level can be followed by particular attachments. The maximum current applied can be

increased up to 400 A. Electricity source: 400 V, 3 phase / 50/60 Hz. or 230 V, 1-phase 50/60 Hz

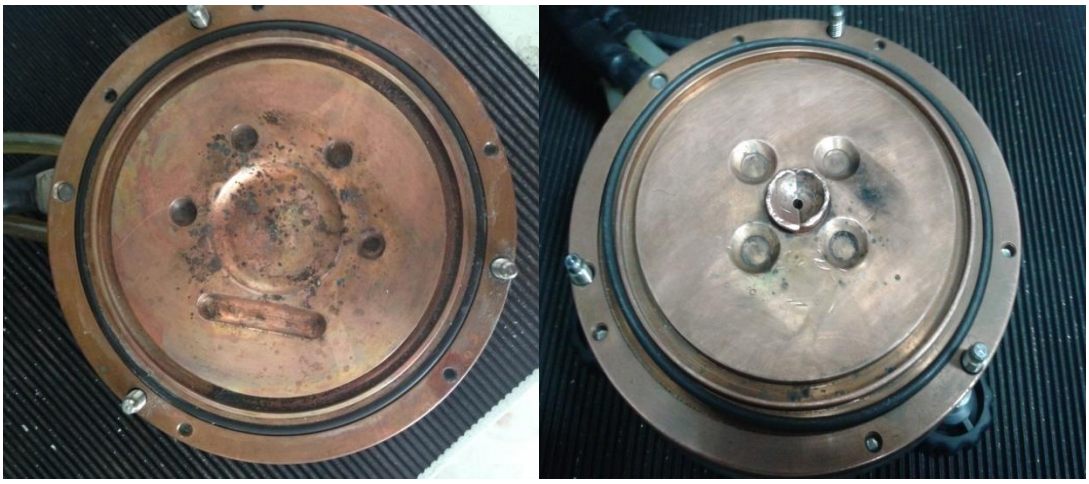

Figure 3.4: Copper crucibles arc melting (left) arc melting and suction casting (right) of mini arc melter

Figure 3.5: Edmund Buehler Arc Melter

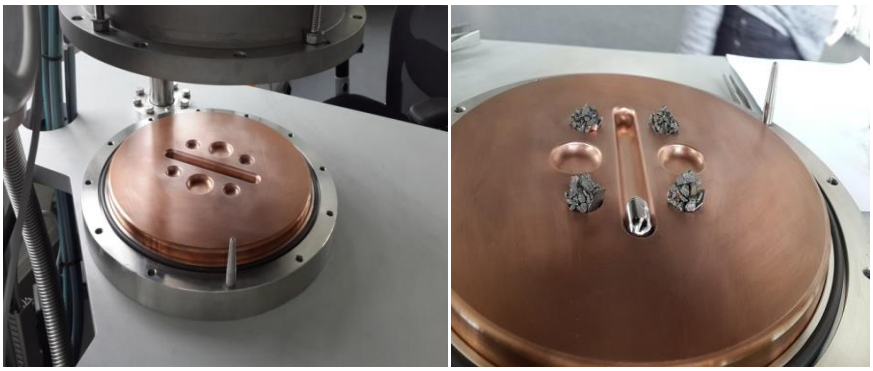

Figure 3.6: Copper crucible for arc melter

3.3 The Materials Used

Three different groups of materials were used in different experiments.

Table 3.1 First group of starting materials

Metal	Purity	Brand
Zr	99.5% bar	Alfa Aesar
Ni	99.8% powder	Alfa Aesar
Cu	99.5% powder	Alfa Aesar
Al	99.8% powder	Alfa Aesar
Ti	99.5% powder	Alfa Aesar

Table 3.2 Second group of starting materials

Metal	Purity	Brand
Zr	99.8% metals basis excluding 3-4% Hf	Alfa Aesar
Ni	99.9% powder	Alfa Aesar
Cu	99.9% powder	Alfa Aesar
Al	99.8% powder	Alfa Aesar
Ti	99.9% powder	Alfa Aesar

The materials at Table 3.2 are kept at Powder Processing Laboratory at I.T.U. Faculty of Chemical and Metallurgical Engineering along with Y metal powder mentioned in Table 3.3. The weight measurement was implemented by the scale within the glovebox that had a sensitivity of measuring 0.001 g. The weight measurements of the materials kept outside the glovebox were implemented by scales that has the sensitivity to measure 0.0001 gram.

Table 3.3 Third group of starting materials

Metal	Purity	Brand
Zr	99.8% metals basis excluding 3-4% Hf	Alfa Aesar
Ni	99.9% wire	Alfa Aesar
Cu	99.9% oxygen free rod	Alfa Aesar
Al	99.8% shots	Alfa Aesar
Ti	99.9% bar	Alfa Aesar

Fig 3.7: Glovebox in which second group of starting materials were kept at.

3.4 The Experiments

3.4.1 The experiments carried out by mini arc melter

Each of the experiments in this system were implemented for preparing only one sample.

Table 3.4 Composition of Sample 1 prepared at mini arc melter

%	Zr	Ti	Cu	Ni	Al
Mol %	52.5	5	17.9	14.6	10
Mass %	65.67	15.59	11.75	3.28	3.7
Mass (15.8 g)	10.5 g	0.52 g	2.5 g	1.9 g	0.6 g*

The materials mentioned in Table 3.1 were used for this experiment. Upon preparation of the materials with required ratios and having them placed on the copper crucible of mini arc melter, the air in the system was evacuated and had argon purged respectively melting was carried out in a Zr-gettered atmosphere. O for 8

times and purging was carried out between -1 and 1 bar. And finally, argon with a pressure of 0.7 bar (which corresponds to -0.3 bar at manometer) was purged. Once the arc was formed, the electrode was spinned above the sacrifice Zr getter material with arc power at 3. After 30 seconds, the electrode was moved above the sample with. After melting for 90 seconds the arc was cut off and the operation was carried out twice more after the sample was flipped each time upon melting. (* Though stochiometrically Al must be involved 0.6 grams, it was involved 0.8 grams due to having it partially evaporated because of its low melting point of 660 ^{0}C.)

Figure 3.8 Sample 1 prepared at mini arc melter.

Sample 2:

Table 3.5 Composition of Sample 2 prepared at mini arc melter

%	Zr	Ti	Cu	Ni	Al
Mol %	52.5	5	17.9	14.6	10
Mass %	65.670	15.59	11.75	3.28	3.7
Mass (15.8 g)	10.5 g	0.52 g	2.5 g	1.9 g	0.6 g*

The materials mentioned in Table 3.1 were used for this experiment. The Zr bar was cut is required amount by Labotom Struers 5 cutter. Upon preparation of the materials with required ratios and having them placed on the copper crucible of mini arc melter, the air in the system was evacuated and had argon purged respectively 8 times. Melting was carried out in a Zr-gettered atmosphere and purging was carried out between -1 and 1 bar. And finally, argon with a pressure of 0.7 bar (which

corresponds to -0.3 bar at manometer) was purged. Once the arc was formed, the electrode was spinned above the sacrifice Zr getter material with arc power at 3. After 30 seconds, the electrode was moved above the sample. Melting was carried out with an arc power that varied between 5-8 power degrees. After melting for 90 seconds the arc was cut off and the operation was carried out twice more after the sample was flipped each time after the melting. (* Though stochiometrically Al must be involved 0.6 grams, it was involved 0.8 grams due to having it partially evaporated because of its low melting point of 660 $^{\circ}$C.)

Figure 3.9 Sample 2 prepared at mini arc melter.

Sample 3:

Table 3.6 Composition of Sample 3 prepared at mini arc melter

%	Zr	Ti	Cu	Ni	Al
Mol %	52.5	5	17.9	14.6	10
Mass %	65.670	15.59	11.75	3.28	3.7
Mass (15.8 g)	10.5 g	0.52 g	2.5 g	1.9 g	0.6 g*

The materials mentioned in Table 3.2 were used for this experiment. Following the preparation of the materials with required ratios and having them placed on the copper crucible of mini arc melter, the air in the system was evacuated and had argon purged respectively for 8 times. Evacuating and purging was carried out between -1 and 1 bar. And finally, argon with a pressure of 0.7 bar (which corresponds to -0.3 bar at manometer) was purged. Melting was carried out in a Zr-gettered atmosphere.

Once the arc was formed, the electrode was spinned above the sacrifice Zr-based getter material with arc power at 3. After 30 seconds, the electrode was moved above the sample. Melting was carried out with an arc power that varied between 5-8 power degrees. After melting for 90 seconds the arc was cut off and the operation was carried out twice more after the sample was flipped each time after the melting. (* Though stochiometrically Al must be involved 0.6 grams, it was involved 0.8 grams due to having it evaporated because of its low melting point of 660 ^{0}C.)

Figure 3.10 Sample 3 prepared at mini arc melter.

Sample 4:

After having button sample synthesized in experiement 1, a part of it that weighs 2.5 grams was cut by Struers Labotom 5 cutter with a SiC disc. It was placed on the rod casting crucible and Zr-based getter material was placed in the sample places near it. Upon preparation of the materials with required ratios and having them placed on the copper crucible of mini arc melter, the air in the system was evacuated and had argon purged respectively for 8 times. Evacuating and purging was carried out between -1 and 1 bar. And finally, argon with a pressure of 0.7 bar (which corresponds to -0.3 bar at manometer) was purged. Melting was carried out in a Zr-gettered atmosphere. Once the arc was formed, the electrode was spinned above the sacrifice Zr-based getter material with arc power at 3. After 30 seconds, the electrode was moved by spinning above the sample. After providing a complete liquefaction the sample was forced to suction casting by opening suction valve of the system. It was seen that the

liqefied alloy melt was spread among the copper parts. The reason behind this was assumed to have a pressure higher than necessary that would prevent a rod form in its entirety become obtained due to the high differential that the extreme pressure difference between the chamber and the crucible caused.

Figure 3.11: Sample 4 prepared at mini arc melter

Sample 5:

After having button sample synthesized in experiment 1, a part of it that weighs 2.5 grams was cut by Struers Labotom 5 cutter with a SiC disc. It was placed on the rod casting crucible and Zr-based getter material was placed in the sample places near it. Upon preparation of the materials with required ratios and having them placed on the copper crucible of mini arc melter, the air in the system was evacuated and had argon purged respectively for 8 times. Evacuating and purging was carried out between -1 and 1 bar. And finally, argon with a pressure of 0.5 bar (which corresponds to -0.5 bar at manometer) was purged. Melting was carried out in a Zr-gettered atmosphere. Once the arc was formed, the electrode was spinned above the sacrifice Zr-based getter material with arc power at 3. After 30 seconds, the electrode was moved by spinning above the sample. After providing a complete liquefaction the sample was forced to suction casting by opening suction valve of the system. It was seen that the liqefied alloy melt was less spread among the copper parts which showed that 0.5 bar

is an applicable value for the process. It also indicated that the alloy melt had a lowe viscosity than it was required.

Figure 3.12: Sample 5 prepared at mini arc melter

Sample 6:

After having button sample synthesized in experiement 1, a part of it that weighs 2.5 grams was cut by Struers Labotom 5 cutter with a SiC disc. It was placed on the rod casting crucible and Zr-based getter material was placed in the sample places near it. Upon preparation of the materials with required ratios and having them placed on the copper crucible of mini arc melter, the air in the system was evacuated and had argon purged respectively for 8 times. Evacuating and purging was carried out between -1 and 1 bar. And finally, argon with a pressure of 0.5 bar (which corresponds to -0.5 bar at manometer) was purged. Melting was carried out in a Zr-gettered atmosphere. Once the arc was formed, the electrode was spinned above the sacrifice Zr-based getter material with arc power at 3. After 30 seconds, the electrode was moved by spinning above the sample. After providing a complete liquefaction the sample was forced to suction casting by opening suction valve of the system. There was no spreading among the copper parts which reveals the fact that viscosity of the alloy melt was at its optimum value.

3.4.2 The experiments carried out by arc melter

Samples 1 and 2 were placed together at the crucible for melting steps to be implemented respectively. Followingly, samples 3,4,5 and 6 were placed together and prepared respectively at the same medium.

Figure 3.13: Sample 6 prepared at mini arc melter

Sample 7:

Table 3.7 Composition of Sample 7 prepared at arc melter

%	Zr	Ti	Cu	Ni	Al
Mol %	52.5	5	17.9	14.6	10
Mass %	65.670	15.59	11.75	3.28	3.7
Mass (15.8 g)	10.5 g	0.52 g	2.5 g	1.9 g	0.6 g*

The arc melter at BOREN was used. The materials mentioned at Table 3.2 were used.After locating the samples in the chamber, the system was evacuated and argon was purged between -1 bar and 1 bar. This step was repeated 3 times. Before argon was purged for the last time, the vacuum level was measured to be at 10^{-6} mbar level. The atmosphere was Ti-gettered. After initiating the arc, electrode was moved towards the getter firstly for 30 seconds. Melting was carried out for approximately for 90 seconds and then the sample was flipped. The current value applied varied

between 180A to 400A to achieve complete melting. After having repeated this step for 3 times, the sample was removed.

Because of the fact that the electrode of this arc melter was incapable of being moved roundly, powders in the composition were spreading around partially and were not able to be involved in the composition (*Though stochiometrically Al must be involved 0.6 grams, it was involved 0.8 grams due to having it partially evaporated because of its low melting point of 660 $^{\circ}$C.)

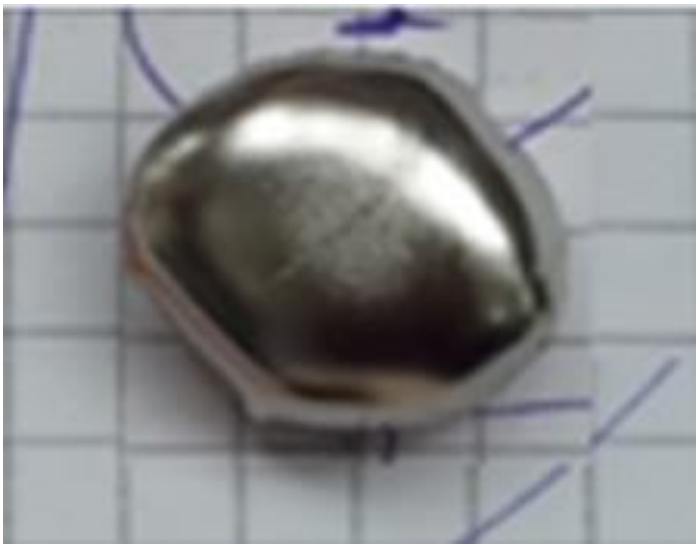

Figure 3.14: Sample 7 prepared at arc melter

Sample 8:

Table 3.8 Composition of Sample 8 prepared at arc melter

%	Zr	Ti	Cu	Ni	Al
Mol %	52.5	5	17.9	14.6	10
Mass %	65.670	15.59	11.75	3.28	3.7
Mass (15.8 g)	10.5 g	0.52 g	2.5 g	1.9 g	0.6 g*

The arc melter at BOREN was used. The materials mentioned at Table 3.2 were used. After locating the samples in the chamber, the system was evacuated and argon was purged between -1 bar and 1 bar. This step was repeated 3 times. Before argon was purged fort he last time, the vacuum level was measured to be at 10^{-6} mbar level. The atmosphere was Ti-gettered. Afterinitiating the arc, electrode was moved towards the getter firstly for 30 seconds. Melting was carried out for approximately for 90 seconds and then the sample was flipped. The current value applied varied between 180A to 400A to achieve complete melting. After having repeated this step for 3 times, the sample was removed.

Because of the fact that the electrode of this arc melter was incapable of being moved roundly, powders in the composition were spreading around partially. (* Though stochiometrically Al must be involved 0.6 grams, it was involved 0.8 grams due to having it partially evaporated because of its low melting point of 660 $^{\circ}$C.)

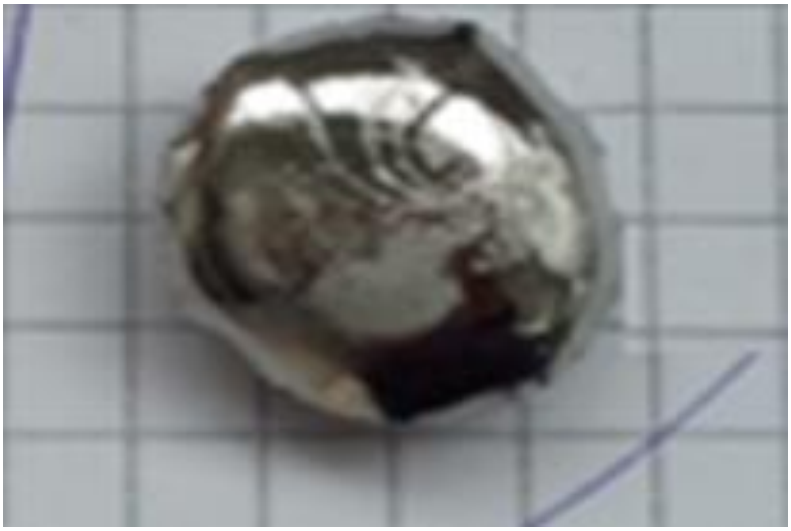

Figure 3.15: Sample 8 prepared at arc melter

Sample 9:

Table 3.9 Composition of Sample 9 prepared at arc melter

%	Zr	Ti	Cu	Ni	Al	Y
Mol %	52.5	5	17.9	14.6	10	0.3
Mass %	65.670	15.59	11.75	3.28	3.7	0. 0001
Mass (15.8 g)	5.25 g	0.26 g	1.25 g	0.95 g	0.4 g*	Appx. 0.0003 g

The arc melter at BOREN was used. The cutting process for preparing bulky materials fort he experiment were carriout out by Struers Accutom 5 diamond cutter. The materials mentioned at Table 3.3 were used. After locating the samples in the chamber, the system was evacuated and argon was purged between -1 bar and 1 bar. This step was repeated 3 times. Before argon was purged fort he last time, the vacuum level was measured to be at 10^{-6} mbar level. The atmosphere was Ti-gettered. Afterinitiating the arc, electrode was moved towards the getter firstly for 30 seconds. Melting was carried out for approximately for 90 seconds and then the sample was flipped. The current value applied varied between 180A to 400A to achieve complete melting. After the first melting step, the chamber was dismantled

and the crucible was cleaned with alcohol. Then, the samples were placed again and the evacuation and purging steps were repeated. Following the sixth melting, a crack in te sample formed during cooling. Remelting upon flipping the sample was carried one more time. (* Though stochiometrically Al must be involved 0.6 grams, it was involved 0.8 grams due to having it partially evaporated because of its low melting point of 660 $^{\circ}$C.)

Figure 3.16: Sample 9 prepared at arc melter

Sample 10:

Table 3.10 Composition of Sample 4 prepared at arc melter

%	Zr	Ti	Cu	Ni	Al	Y
Mol %	52.5	5	17.9	14.6	10	0.8
Mass %	65.670	15.59	11.75	3.28	3.7	0. 00027
Mass (15.8 g)	5.25 g	0.26 g	1.25 g	0.95 g	0.4 g*	Appx. 0.0008 g

The arc melter at BOREN was used. The materials mentioned at Table 3.3 were used. The cutting process for preparing bulky materials fort he experiment were carried out out by Struers Accutom 5 diamond cutter. After locating the samples in the chamber, the system was evacuated and argon was purged between -1 bar and 1 bar. This step was repeated 3 times. Before argon was purged fort he last time, the vacuum level was measured to be at 10^{-6} mbar level. The atmosphere was Ti-gettered. After initiating the arc, electrode was moved towards the getter firstly for 30 seconds. Melting was carried out for approximately for 90 seconds and then the sample was flipped. The current value applied varied between 180A to 400A to achieve complete melting. Just before the sample was to be flipped over, it cracked upon cooling. Followingly, the chamber was dismantled and the crucible was cleaned

with alcohol. Then, the samples were placed again and the evacuation and purging steps were repeated Remelting upon flipping the sample was carried out 5 more times.(* Though stochiometrically Al must be involved 0.6 grams, it was involved 0.8 grams due to having it partially evaporated because of its low melting point of 660 $^{\circ}$C.)

Figure 3.17: Sample 10 prepared at arc melter

Sample 11:

Table 3.11 Composition of Sample 5 prepared at arc melter

%	Zr	Ti	Cu	Ni	Al	Y
Mol %	52.5	5	17.9	14.6	10	0.6
Mass %	65.67	15.59	11.75	3.28	3.7	0. 0002
Mass (15.8 g)	5.25 g	0.26 g	1.25 g	0.95 g	0.4 g*	Appx. 0.0006 g

The arc melter at BOREN was used. The materials mentioned at Table 3.3 were used. The cutting process for preparing bulky materials fort he experiment were carried out out by Struers Accutom 5 diamond cutter. After locating the samples in the chamber, the system was evacuated and argon was purged between -1 bar and 1 bar. This step was repeated 3 times. Before argon was purged fort he last time, the vacuum level was measured to be at 10^{-6} mbar level. The atmosphere was Ti-gettered. Afterinitiating the arc, electrode was moved towards the getter firstly for 30 seconds. Melting was carried out for approximately for 90 seconds and then the sample was flipped. The current value applied varied between 180A to 400A to achieve complete melting. After the first melting step, the chamber was dismantled and the crucible was cleaned with alcohol based solution. Then, the samples were placed again and the evacuation and purging steps were repeated. Following the

second melting, a crack in te sample formed during cooling. Remelting upon flipping the sample was carried out 4 more times. (* Though stochiometrically Al must be involved 0.6 grams, it was involved 0.8 grams due to having it partially evaporated because of its low melting point of 660 $^{\circ}$C.)

Figure 3.18 Sample 11 prepared at arc melter

Sample 12:

Table 3.12 Composition of Sample 6 prepared at arc melter

%	Zr	Ti	Cu	Ni	Al	Y
Mol %	52.5	5	17.9	14.6	10	0.7
Mass %	65.67	15.59	11.75	3.28	3.7	0. 00023
Mass (15.8 g)	5.25 g	0.26 g	1.25 g	0.95 g	0.4 g*	Appx. 0.0007 g

The arc melter at BOREN was used. The materials mentioned at Table 3.3 were used. The cutting process for preparing bulky materials for the experiment were carried out out by Struers Accutom 5 diamond cutter was used. After locating the samples in the chamber, the system was evacuated and argon was purged between -1 bar and 1 bar. This step was repeated 3 times. Before argon was purged fort he last time, the vacuum level was measured to be at 10^{-6} mbar level. The atmosphere was Ti-gettered. After initiating the arc, electrode was moved towards the getter firstly for 30 seconds. Melting was carried out for approximately for 90 seconds and then the sample was flipped. The current value applied varied between 180A to 400A to achieve complete melting. After the first melting step, the chamber was dismantled and the crucible was cleaned with alcohol. Then, the samples were placed again and the evacuation and purging steps were repeated. Remelting upon flipping the sample was carried 5 more times. (* Though stochiometrically Al must be involved 0.6

grams, it was involved 0.8 grams due to having it partially evaporated because of its low melting point of 660 $^{\circ}$C.)

Figure 3.19: Sample 12 prepared at arc melter

3.5 Characterization Studies

3.5.1 Optical microscopy

As amorhous structure formation is expected to form at the center of the samples,for metallography analyses, the samples prepared at the arc melter at BOREN were cut into two halves by Struers Labotom 5 SiC cutter. One half of each of them were subjected to hot bakalite and cooled afterwards. Followingly, grinding for each of them by SiC papers with 400, 800, 1200, 1800 and 2500 grit numbers were carried out. Subsequently, polishing was implemented by three different polishing solutions including 9 mm, 6 mm and 3 mm diamond pieces. Finally the samples were etched with a solution that consisted of 90%HNO_3(65%) and 10%HF (35%) and were examined by Olympos Optical Microscope with 100 times magnification scoping 10 micron length magnitude.

3.5.2 XRD analyses

The samples mentioned section 3.3.2.1 were unseen. For XRD studies, the equipment used was at İ.T:Ü Prof. Dr. Adnan Tekin Materials Science Application and Research Center. The brand and model of the equipment is Panalytical PW3040/60. Copper is the anode material and the X-ray scanning angle was 10-90. 45 kV -40 mA power is applied. X2Pert HighScore Plus 2.2b programme is used for phase analyses.

4. RESULTS AND DISCUSSION

4.1 Visual Inspection

A very rapid cooling that occurred approximately in ten seconds was observed for each of the samples due to the high cooling rates of the prepared alloys which was asserted to be 10-15 Ks^{-1}(Lin, Johnson and Rhim, 1996).

Upon crack formations observed at samples 2, 3 and 5 synthesized at the arc melter at BOREN, it was seen that the crack surface had a brittle structure which that indicates crystallization took place in alloy. In order to eliminate that factor remelting steps were carried out with applying high current values (up to 400 A).

As clinks and scratches on the copper mold surface act as nucleation sites (Peker, 1994), the crack formations occurred due to propagation.

All the samples synthesized had a shiny and lustrous surface which is assumed as the primary visual property of amorphous metal alloys.

4.2 Chemical Analysis

Three pieces of sample 1 which was synthesized at the mini arc melter were cut by Struers Labotom 5 SiC cutter. They were cast as rods by suction casting and following having small pieces of them cut by SiC cutter, they were subjected to atomic absorption analysis. The results are shown at the table below:

Table 4.1 Atomic absoption analysis of Zr BMG

Sample pieces	Cu%	Ni%	Al%	Ti%
Ideal	15.59	11.75	3.28	3.7
1.1	14.93	12.46	3.79	3.95
1.2	15.00	13.64	3.81	3.64
1.3	15.0	11.76	3.64	3.63

As variations between the prepared alloy composition and the composition of the product synthesized are oftenly encountered in experiments carried out by arc melters, differences between the ideal ratios and experimentals results were observed

(Kündig, 2002) . However, addition of excess Al (33% more than the stochiometric value) had been helpful at obtaining results similar to what was intended to be obtained. Other reasons may include having powders fly about because of the power of the arc or mistakes in sensitive weight measurements.

Five pieces of sample 2 which was synthesized at the mini arc melter were cut by Struers Labotom 5 SiC cutter. They were cast as rods by suction casting and following having small pieces of them cut by SiC cutter, they were subjected to oxygen content analysis by LECO analyzer. The results are shown at the table below:

Table 4.2 Oxygen Content Analysis of Zr BMG

Sample pieces	Mass% Oxygen Contents
2.1	0.0332
2.2	0.0299
2.3	0.229
2.4	0.465
2.5	0.229

According to studies carried out by Kündig et al. (2002) in case the oxygen content in a bulk metallic glass rod 3 mm in diameter exceeded approximately 120 ppm, crystallization could not be hindered and cause decreasing the possibility of obtaining full amorphization for the sample.

4.3 XRD Results

Arc melting process shows parallelism to conventional casting of alloys in a metal mold (Abbaschian, 2009). The solidification microstructure in a conventional cast alloy can be is examined as three types. The first type that is in direct contact with the mold wall would have experienced a very high undercooling. Consequently, the nucleation rate is very high and therefore, the “chill” zone, consisting of extremely fine grains, is formed. Following this, one will have a columnar structure due to the presence of an inverse temperature gradient in the liquid ahead of the solid/liquid interface. The last type will be the formation of equiaxed structure again due to the occurrence of constitutional supercooling in alloys. In the case of arc-cast alloys also, one can visualize these three different zones of solidification. However, if bulk metallic glasses are being scoped, instead of the central equiaxed zone, we could have the glassy phase region in the center of the ingot. As glass formation is

expected to take place at the central region in order to see the difference in structure formation both surface and inner region XRD analyses were taken into account

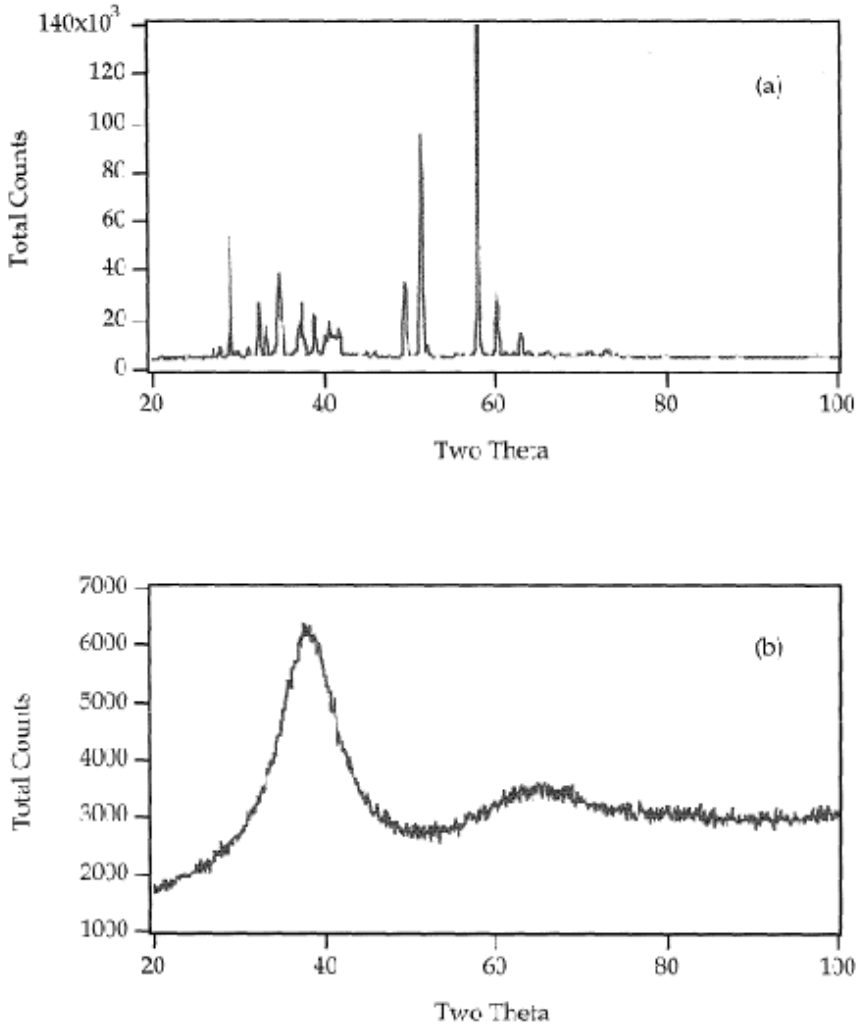

Figure 4.1: X-ray diffraction patterns taken from various parts of a 6 gram ingot of $Zr_{41.2}Ti_{13.8}Cu_{17.9}Ni_{10.0}Be_{22.5}$ bottom surface where contact with silver boat occurs and (b) cross section surface parallel to the plane of the silverboat surface the melting was carried out (Peker, 1994).

.

In the figure, the difference between the phases formed on the surface in contact with the melt and cross section surface paralel to the plane of the silverboat surface can be seen.

4.3.1 XRD analyses for Zr-BMG rod

XRD analyses for samples 5 and 6 which were synthesized at mini arc melter and had a composition of $Zr_{52.5}Cu_{17.9}Ti_5Ni_{14.6}Al_{10}$ was carried out for surface and inner region of the sample.

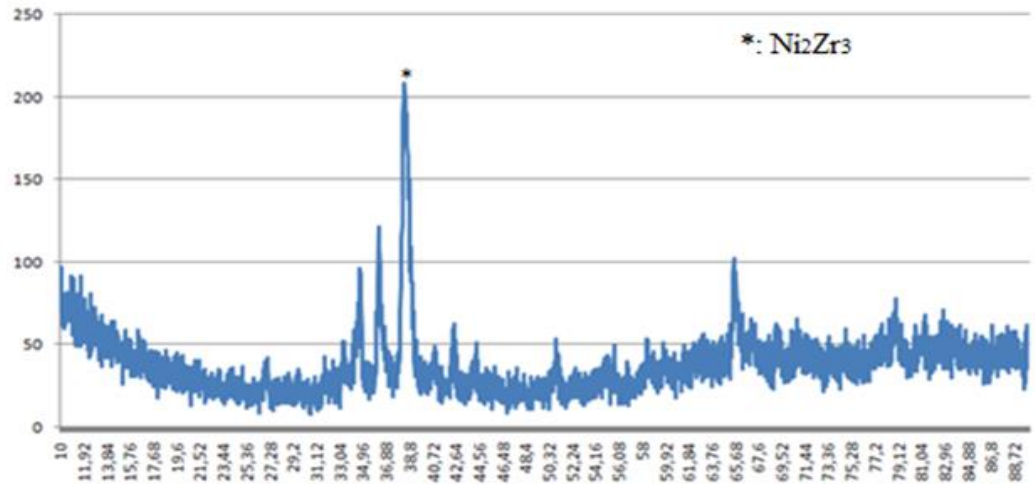

Figure 4.2: Surface of Zr-BMG rod

Formation of Ni_2Zr_3 phase was observed which prevented amorphization on the surface.

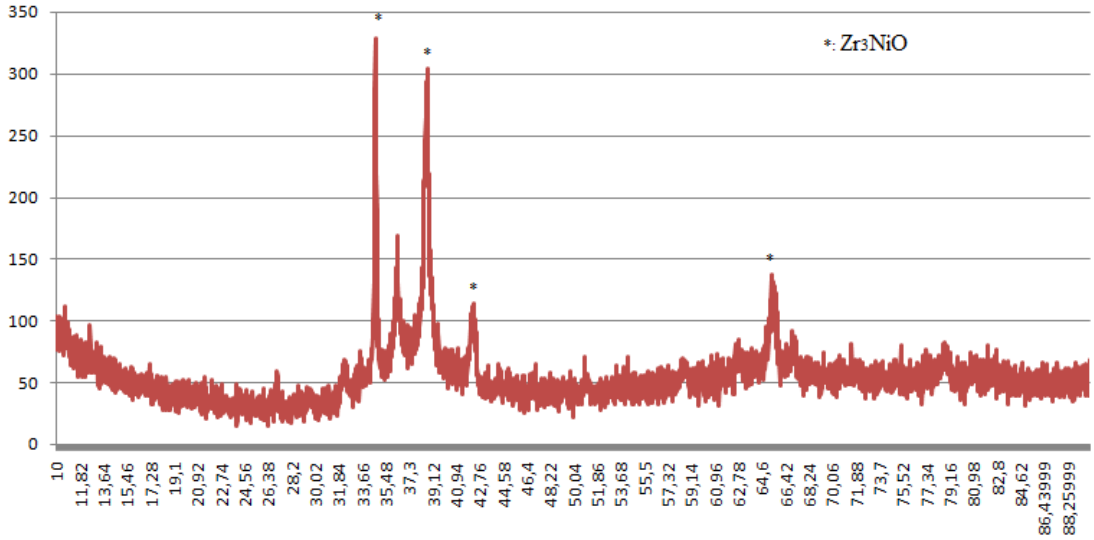

Figure 4.3: Inner region of Zr-BMG rod

Inner region of Zr-BMG, it was seen that Zr3NiO phase had formed in the iner region. Cheng et. Al (2013) suggests that oxygen is segregated in the precipitated Zr_3NiO-type and β-Zr crystals in Zr based BMGs with compositions of $Zr_{41.2}Ti_{13.8}Cu_{12.5}Ni_{10}Be_{22.5}$ and $Zr_{39.6}Ti_{33.9}Nb_{7.6}Ni_{6.4}Be_{12.5}$ which results in releasing

amorphous matrix by making a composite with a metallic glass matrix. Regarding this analysis, it can be claimed that same kind of segregation tends to occur at $Zr_{52.5}Cu_{17.9}Ni_{14.6}Ti_5Al_{10}$ alloy.

4.3.2 XRD analyses for button samples

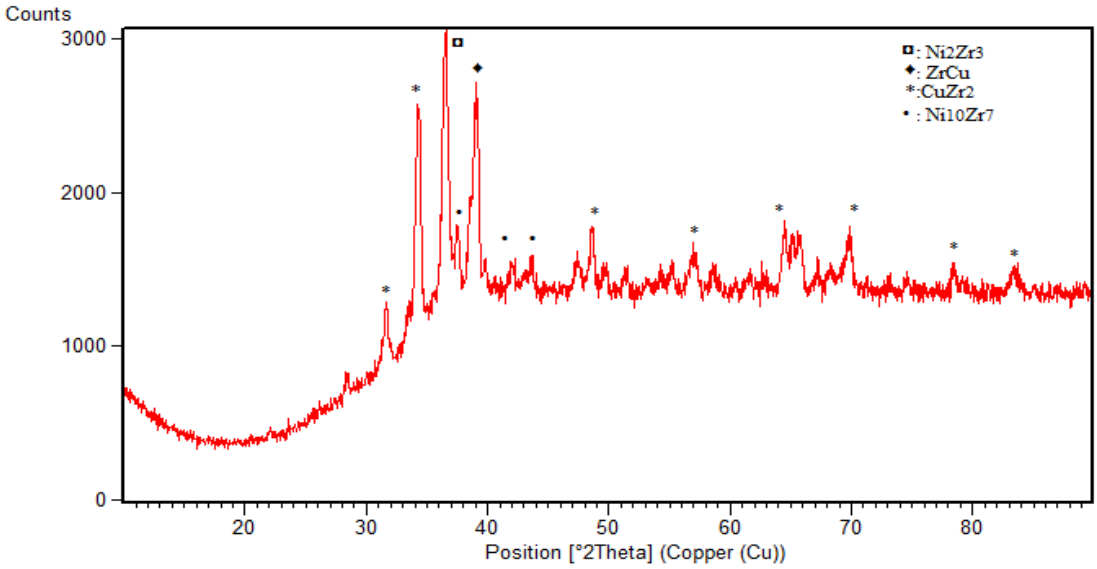

Figure 4.4: XRD analyses of Sample 3.

Results for Sample 3 are shown in figure 4.Along with partial amorphization phases $CuZr_2$and ZrCu phases form which lead to heterogeneous nucleation. Intermetallic $Ni_{10}Zr_7$ was also seen to have formed as a result of crystallization. Ni_2Zr_3 takes place among the phases formed.

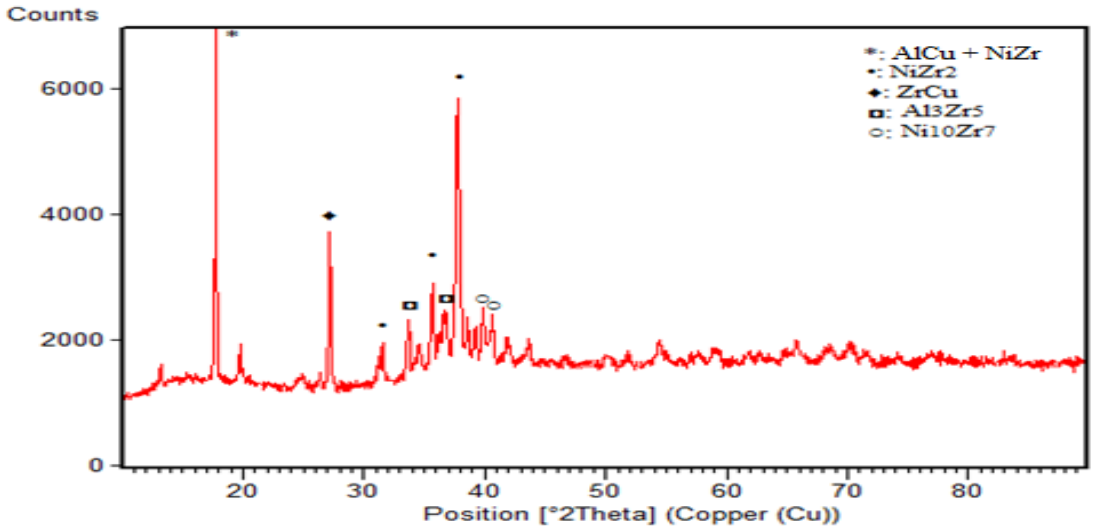

Figure 4.5: XRD analyses of Sample 7.

Results for sample 7 is shown in figure 4.3.Partial amorphization is seen. $NiZr_2$, NiZr and ZrCu phases form which lead to full heterogeneous nucleation. Al_3Zr_5 phase which was claimed to form as a consequence of yttrium addition by Gebert et al.(1998), was seen to have formed in Hf including Vit105 alloy. Intermetallic $Ni_{10}Zr_7$ was also seen to have formed as a result of crystallization

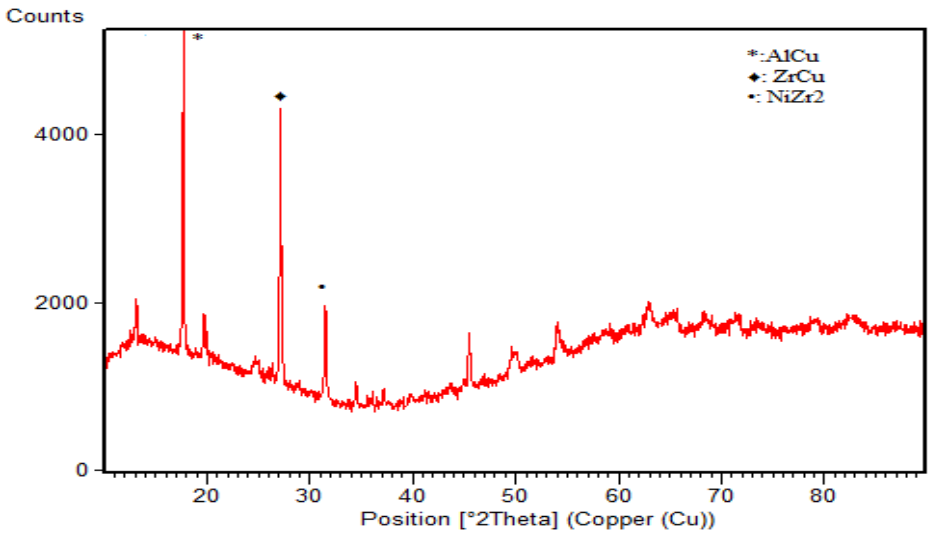

Figure 4.6:XRD analyses of Sample 8.

Results for sample 8 is shown in figure 4.4.Besides ZrCu and NiZr and AlCu phases form which lead to full heterogeneous nucleation. Amorphization is more dominant compared to other samples.

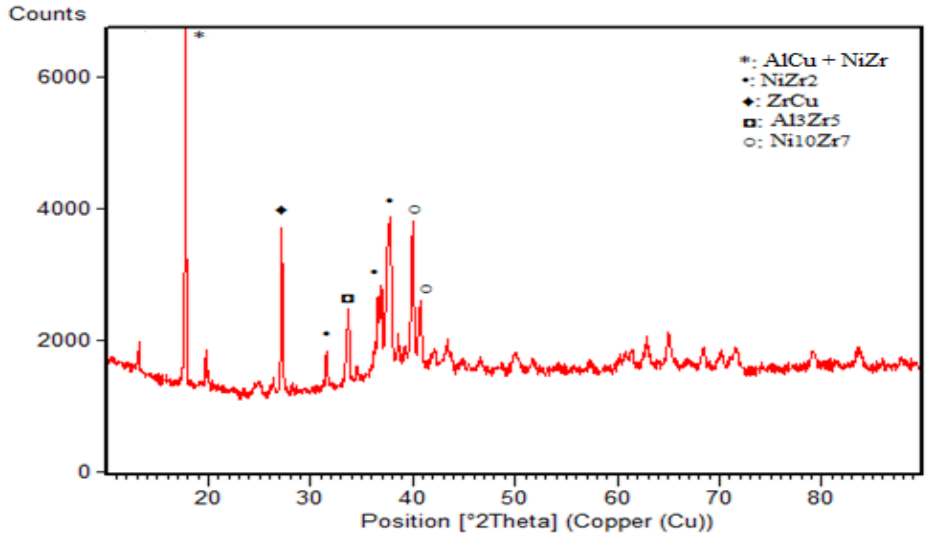

Figure 4.7: XRD analyses of Sample 9.

Results for sample 9 is shown in figure 4.5.Intermetallics $NiZr_2$, NiZr and ZrCu phases form which lead to full heterogeneous nucleation. Al_3Zr_5 phase which was claimed to form as a consequence of yttrium addition by Gebert et al. (1998), was seen to have formed in Hf including Vit105 alloy. $Ni_{10}Zr_7$ was also seen to have formed as a result of crystallization.

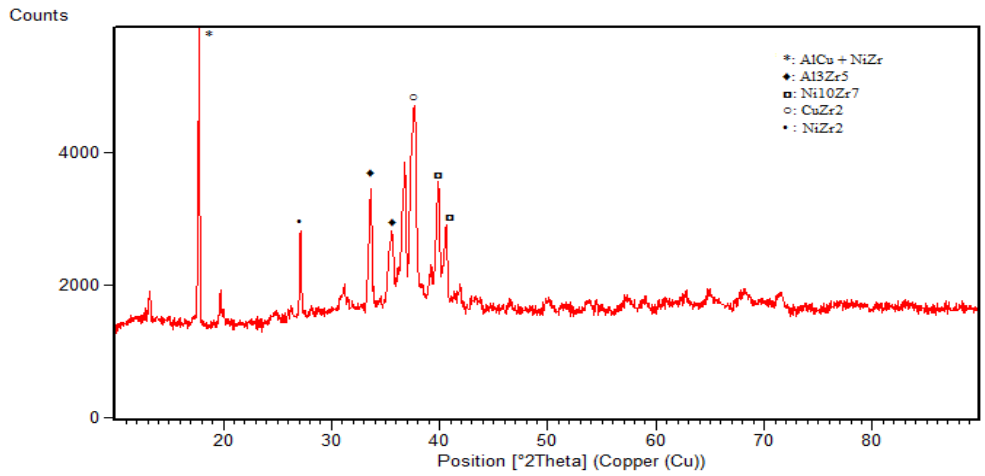

Figure 4.8: XRD analyses of Sample 10.

Results for sample 10 is shown in figure 4.6. $NiZr_2$, NiZr and $CuZr_2$ phases form which lead to full heterogeneous nucleation. Al_3Zr_5 phase which was claimed to form as a consequence of yttrium addition by Gebert et al. (1998), was seen to have formed in Hf including Vit105 alloy. Intermetallics $Ni_{10}Zr_7$ was also seen to have formed as a result of crystallization

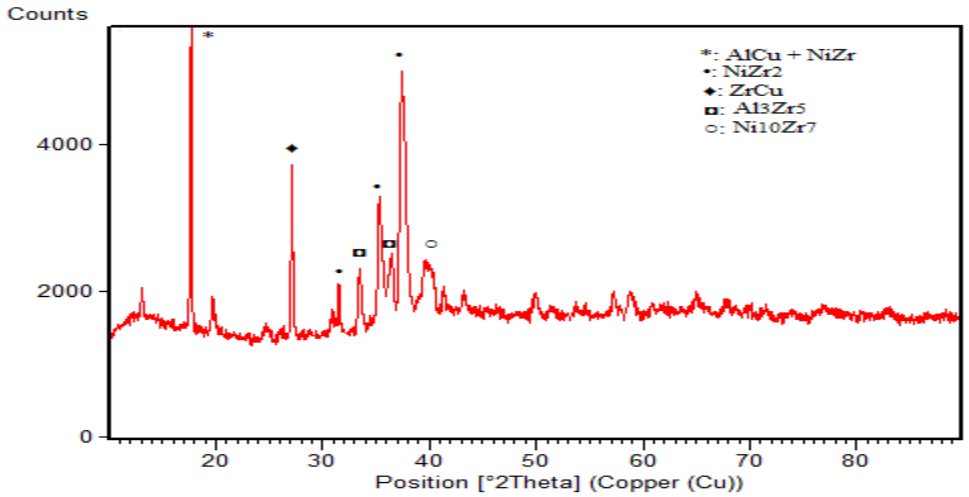

Figure 4.9: XRD analyses of Sample 11.

Results for sample 11 is shown in figure 4.6.Along with partial amorphization phases $NiZr_2$, NiZr and ZrCu phases form which lead to full heterogeneous nucleation. Al_3Zr_5 phase which was claimed to form as a consequence of yttrium addition by Gebert et al. (1998), was seen to have formed in Hf including Vit105 alloy. Intermetallics $Ni_{10}Zr_7$ was also seen to have formed as a result of crystallization

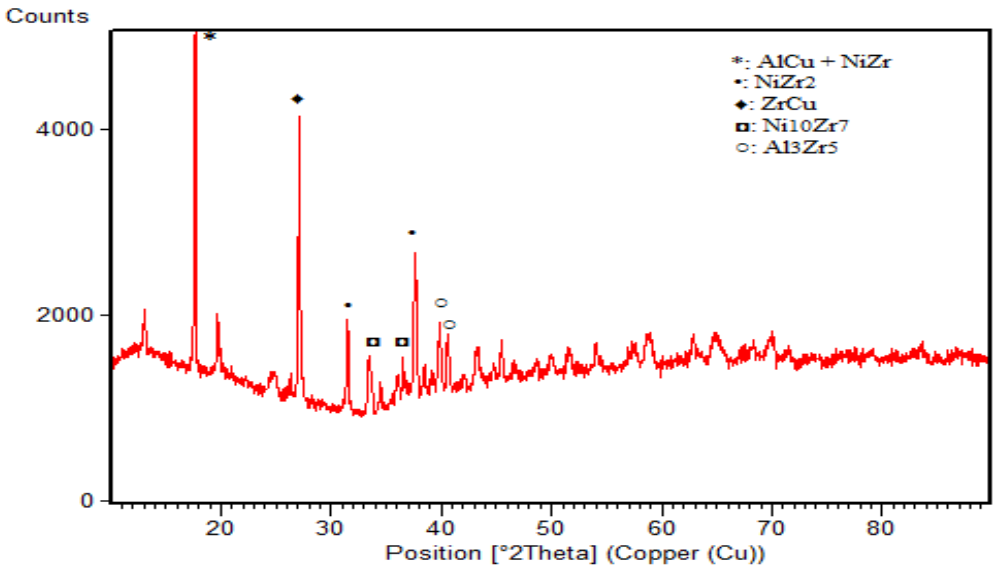

Figure 4.10: XRD analyses of Sample 12.

Results for sample 12 is shown in figure 4.7.Along with partial amorphization phases $NiZr_2$, NiZr and ZrCu phases form which lead to full heterogeneous nucleation. Al_3Zr_5 phase which was claimed to form as a consequence of yttrium addition by Gebert et al., was seen to have formed in Hf including Vit105 alloy. Intermetallics $Ni_{10}Zr_7$ was also seen to have formed as a result of crystallization.

4.4 Metallography Results

If bulk metallic glasses are being scoped, instead of the central equiaxed zone which is seen at conventionally cast alloys, we could have the glassy phase region in the center of the ingot. In metallography studies, it is quite significant that a glassy phase forms in the inner region where the heat flux reinforced from the copper hearth disappears and the cooling rate is reduced. This low cooling rate is sufficient for some of the alloys to become glassy(Inoue, 2011). But, it is a known fact that preventing heterogeneous nucleation in this systems to occur is very rare.

Sample 7

Figure 4.11: Optical microscopy image of Sample 7 (100x)

Dendrite formation due to phase segregation was seen in the structure as a result of rapid cooling. The reason that caused that to happen was having powder flown about as the electrode of the system could not be spinned above the sample having the powder molten along with the bulk materials.

Sample 8

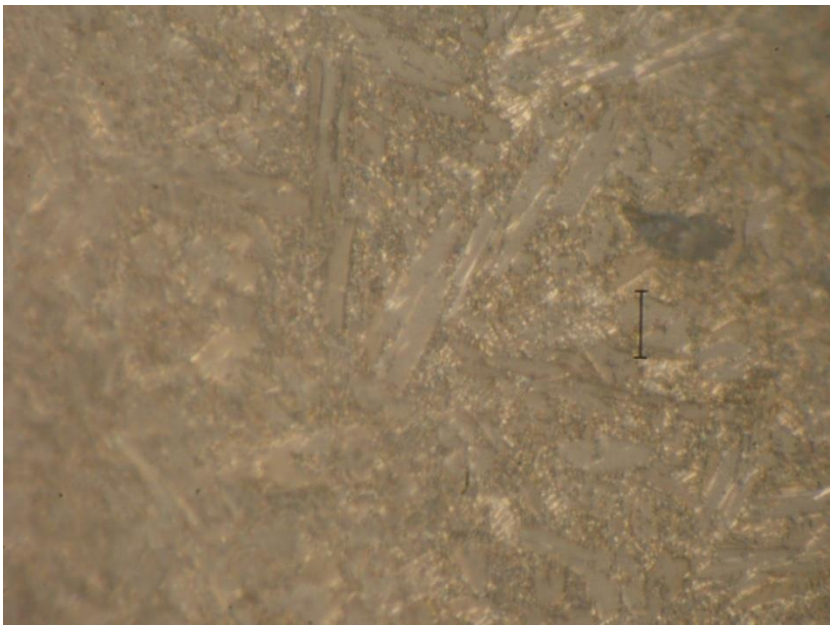

Figure 4.13: Optical microscopy image of sample 8 (100x)

Formation of small grains along with partial amorphization is seen. Although powder materials were used as starting materials dendrite formation is not seen as in samples 7 and 9.

Sample 9

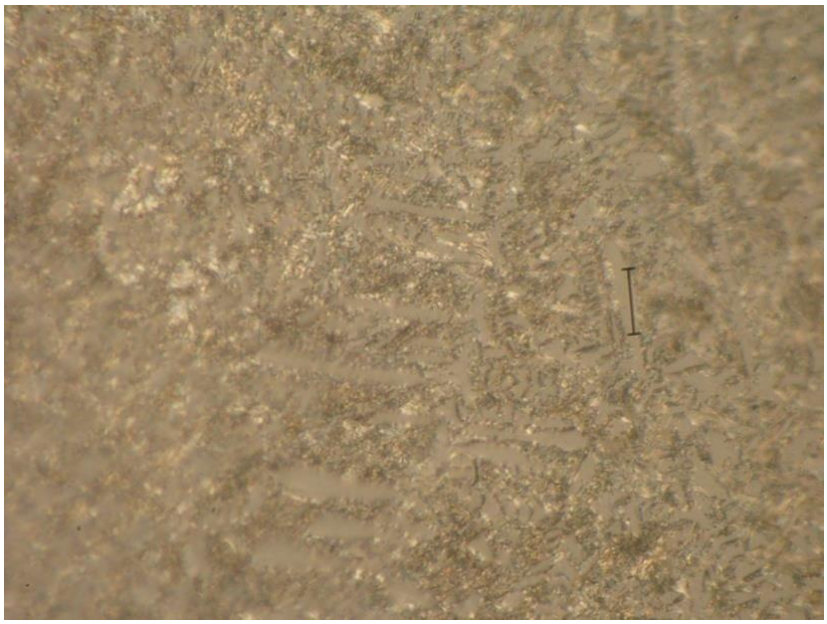

Figure 4.13: Optical microscopy image of Sample 9 (100x)

Though dendrite formation was observed a less significant phase seperation is seen compared to sample 7 due to having yttrium included with an amount of 0.03%.

Sample 10

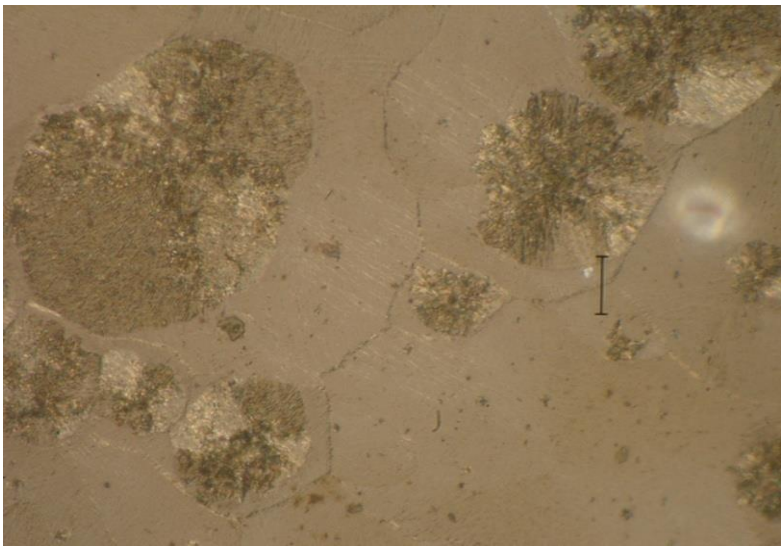

Figure 4.14: Optical microscopy image of Sample 10 (100x)

The effect increasing yttrium up to 0.08% is seen due to obtaining coarser grains and having dendrites eliminated as it acts as an oxygen scavenger in the central region as stabilizing the structure. However effects of rapid cooling are seen as phase segregation instead of amorphization which might lead into crack formation.

Sample 11

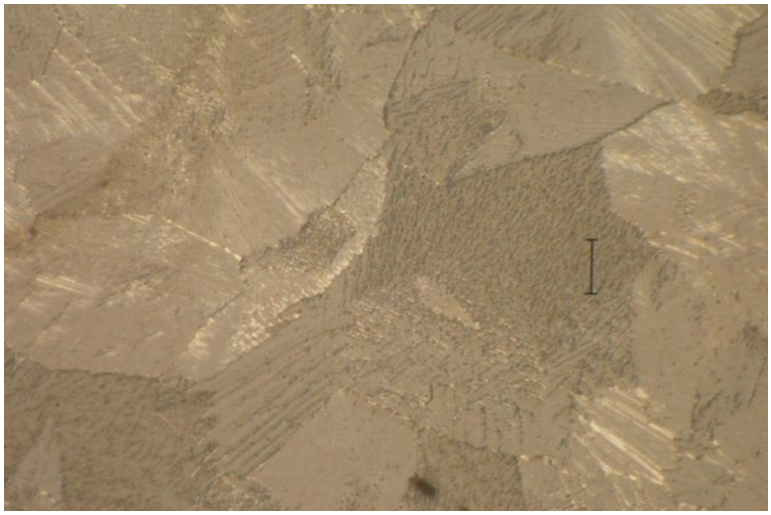

Figure 4.15: Optical microscopy image of Sample 11 (100x)

Grain formation due to crystallization is observed at 0.06% Y addition. Compared to sample 10, the grains are smaller which reveals the fact that more yttrium is required in order to prevent having oxygen distributed freely within the structure which catalyzes crystallization.

Sample 12

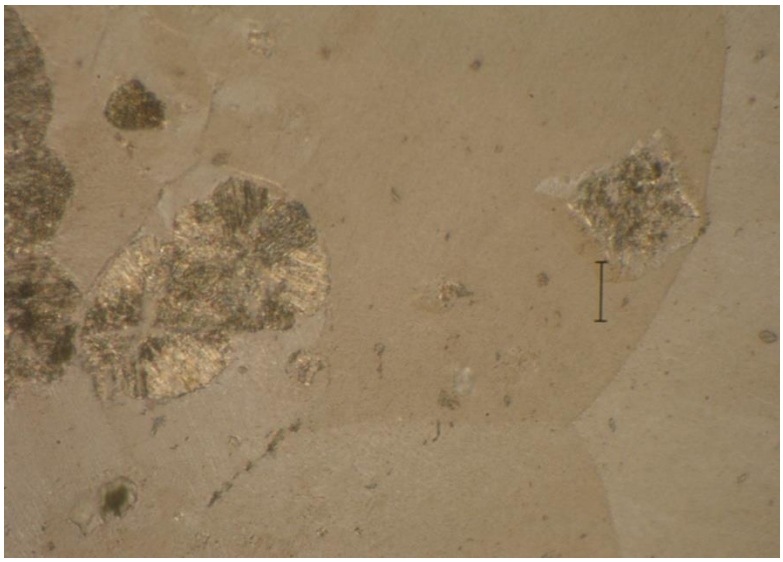

Figure 4.16: Optical microscopy image of Sample 12 (100x)

Scavenging effect of having 0.07% yttrium included is seen due to obtaining a structure that contains coarser grains and having dendrites eliminated in the regions crystallization took place. Regions with partial amorphization with crystal nuclei suspended in the matrix are seen.

5. CONCLUSIONS AND RECOMMENDATIONS

1. In this study, experiments focused on obtaining Vit105, a commercial bulk metallic glass alloy with $Zr_{52.5}Ti_5Ni_{14.6}Cu_{17.9}Al_{10}$ atomic ratio which has a non-toxic composition besides having high mechanical and corrosion properties.

2. As starting materials, in order to observe the differences in results based on them Zr bar with 99.5% purity and for the first time, Zr lumps with 99.8% metal basis containing Hf up to 3-4% were used due to examine the effect of Hf presence in alloy on amorphization as apart from the studies in which high purity Zr and high purity Hf were separately added in Vit105 compositions, in this study Hf used, which seperating from Zr requires a detail-oriented process, took place as a constituent of Zr lumps.

3. In order to examine the effect of oxygen presence in the composition, the effect of addition of yttrium in different ratios as as oxygen scavenger was studied by microalloying, depending on the fact that yttrium and oxygen reacts to form Y_2O_3, setting the glass matrix free.

4. All the experiments were carried out in high purity argon atmosphere with high vacuum values up to 10^{-6} mbar by arc melting along with Ti- and Zr- getters. The samples with following compositions were subjected to remelting for several times in order to obtain complete homogeneity:

- $Zr_{52.5}Ti_5Cu_{17.9}Ni_{14.6}Al_{10}$
- $(Zr_{52.5}Ti_5Cu_{17.9}Ni_{14.6}Al_{10})_{99.7}Y_{0.3}$
- $(Zr_{52.5}Ti_5Cu_{17.9}Ni_{14.6}Al_{10})_{99.6}Y_{0.8}$
- $(Zr_{52.5}Ti_5Cu_{17.9}Ni_{14.6}Al_{10})_{99.2}Y_{0.6}$
- $(Zr_{52.5}Ti_5Cu_{17.9}Ni_{14.6}Al_{10})_{99.3}Y_{0.7}$

5. Visually, all the samples obtained had shiny and lustrous surfaces which implied glass formation.

6. XRD analysis for surface and inner parts of the samples were implemented. Prior to analysis, samples preparation was carried out by SiC and diamond cutters by having samples horizontally cut in order to be able to examine the effect of rapid solidification by detecting phases formed on the surface that was in contact with the copper crucible, the center and the upper surface of the sample. Results revealed that amorphization increased in the central region compared to others. Also, it was seen that in rod sample, as cooling is provided homogeneously throughout the entire structure, crystallization could more successfully be prevented and provide glassy phase become formed.

7. Optical microscopy with 100 times magnification was implemented following grinding, polishing and etching steps respectively. Consequently, the effect of microalloying with yttrium was seen to have dendrites eliminated from the structure and depending on different amounts of addition as it decreases the nucleating effect of oxygen presence by formin Y_2O_3 compound, a structure which restrict heterogeneous nucleation, which tends to make the alloy melt lead to partial amorphization upon rapid cooling.

8. In order to detect the thermal stability of the samples DSC analyses should be carried out in order to detect the glass forming temperature and crystallization temperatures. Effect of oxygen impurity, scavenging effect of yttrium and having Hf combined Zr on thermal behavior of the samples should be analysed.

9. Surfaces of copper molds used must be free of cavities and stretches in order to prevent nucleation in the samples

10. Starting materials must be preferred to be in bulk form in case they are available.

11. Compositions in which Hf is substituted with Zr in ratios such as;

- $(Zr_{(52.5-x)}Hf_xTi_5Cu_{17.9}Ni_{14.6}Al_{10})_{99.7}Y_{0.3}$ (x=0.2)

- $(Zr_{(52.5-x)}Hf_xTi_5Cu_{17.9}Ni_{14.6}Al_{10})_{99.6}Y_{0.4}$ (x=0.4)

- $(Zr_{(52.5-x)}Hf_xTi_5Cu_{17.9}Ni_{14.6}Al_{10})_{99.2}Y_{0.8}$ (x=0.6)

- $(Zr_{(52.5-x)}Hf_xTi_5Cu_{17.9}Ni_{14.6}Al_{10})_{99}Y_1$ (x=0.8) should be prepared and subjected to required analyses.

REFERENCES

Abbaschian, R., L. Abbaschian, and R.E. Reed-Hill (2009). *Physical Metallurgy Principles*, 4th edn. Stamford, CT: CENGAGE Learning.

Barandiaran, J.M. and Colmenero,J. (1981). Continuous cooling approximationfor the formation of a glass. *J. Non-Cryst. Solids* 46: 277–287.

Choi-yim, H., Busch, R. and Johnson, W. L.(1998). The effect of silicon on the bulk metallic glass forming alloy during processing of composites $Cu_{47}Ti_{34}Zr_{11}Ni_8$ *J. Appl.Phys.* 837993

Drehman, A.J., Greer, A.L., and Turnbull, D. (1982). Bulk formation of a metallic glass: Pd40Ni40P20. *Appl. Phys. Lett*. 41: 716–717.

FactSage 6.4 Software, 2011

Fredriksson, H., Akerlind, U. (2012). Solidification and Crystallization Processing in Metals and AlloysISBN: 978-1-119-99305-6*Wiley.*

Gebert, A., Eckert, J., and Schultz, L.(1998).Effect of oxygen on phase formation and thermal stability of slowly cooled $Zr_{65}Al_{7.5}Cu_{17.5}Ni_{10}$ metallic glass. *Acta Mater. 46: 5475–5482.*

Gu, X., Xing, L.Q., and Hufnagel, T.C., (2002). Glass-forming ability and crystallization of bulk metallic glass $(Hf_xZr1-_x)_{52.5}Cu_{17.9}Ni_{14.6}Al_{10}Ti_5$. *J. Non-Cryst. Solids*

Inoue, A. (1998). Bulk Amorphous Alloys: Preparation and Fundamental Characteristics,*Uetikon-Zurich, Switzerland: Trans Tech Publications*.

Inoue, A. and Zhang, T. (1995). Fabrication of bulky Zr-based glassy alloys by

Inoue, A., Kita, K., Zhang, T., and Masumoto, T. (1989). An amorphous La55Al25Ni20 alloy prepared by water quenching. *Mater. Trans., JIM* 30: 722–725.

Inoue, A., Nakamura, T., Nishiyama, N., and Masumoto, T. (1992). Mg–Cu–Y bulk amorphous alloys with high tensile strength produced by a high-pressure die casting method. *Mater. Trans., JIM* 33: 937–945.

Inoue, A., Shinohara, Y., Yokoyama, Y., and MasumotoT. (1995). Solidification analyses of bulky Zr60Al10Ni10Cu15Pd5 glass produced by casting into wedgeshape copper mold. *Mater. Trans., JIM* 36: 1276–1281.

Inoue, A., Yokoyama, Y., Shinohara, Y., and MasumotoT. (1994). Preparation of bulky Zr-based amorphous alloys by a zone melting method. *Mater. Trans., JIM* 35: 923–926.

Jang, F., Wang, Z. J., Zhang Z. B.,and Sun, J. (2005) Formation of Zr-based Bulk Metallic Glasses from Low Purity Materials by Scandium Addition, *Scripta Materialia, Volume 53, Issue 5, September 2005, Pages 487–491.*

Kubaschewski, O. and Alcock, C. B. (1979)**.**Metallurgical Thermochemistry *Pergamon, Oxford.*

Kui, H.W., Greer, A.L., and Turnbull, D. (1984). Formation of bulk metallic glass by fluxing. *Appl. Phys. Lett*. 45: 615–616.

Kundig, A. (2002), *Mater. Trans.* **43** 3206.

Kündig, A., Lepori D., Perry, A., Rossman, S., Blatter, A., Dommann, A., Uggowitzer, P.J. (2002) Influence of Low Oxygen Content and Alloy Refinement on the Glass Forming Ability of Zr52.5Cu17.9Ti5Ni14.6Al10 *Materials Transactions 43:3206-3210.*

Lin, X.H., Johnson, W.L., and Rhim, W.K. (1997).Effect of oxygen impurity on crystallization of an undercooled bulk glass forming Zr–Ti–Cu–Ni–Al alloy. Mater. Trans., JIM 38: 473–477.

Liu C. T., Chisholm M. F . and Miller M. K. (2002).*Intermetallics***10** 1105.

Lu, Z. P. and Liu, C. T. Role of minor alloying additions in formationof bulk metallic glasses: A ReviewJournal of Materials Science 39(2004) 3965 – 3974

Lu, Z. P., Liu, C. T. and Porter, W. D. (2003). , *Appl. Phys. Lett.***83** 2581.

Lynch, R.F.,Olley, R.P.,**and Gallagher P.C.J.** (1975). Squeeze casting of brass

Mei, J.(2009). Titanium-based Bulk Metallic Glasses: Glass Forming Ability and Mechanical Behavior. *Universit´e Joseph-Fourier*.

Men, H., Hu, Z. Q. and Xu, J. (2002)*Scripta Mater*. 46 699.

Miller, M. and Liaw, P. (2008). Bulk Metallic Glasses, *Springer.*

Mukherjee, S. (2005). *Study of crystallization behavior, kinetics and thermodynamics of bulk metallic glasses using noncontact electrostatic levitation technique.* Dissertation (Ph.D.), California Institute of Technology.

Nishiyama, N. and Inoue, A. (2002). Direct comparison between critical cooling rate and some quantitative parameters for evaluation of glass-forming ability in Pd–Cu–Ni–P alloys. *Mater. Trans*. 43: 1913–1917

Nishiyama, N., Takenaka,K., and Inoue,A. (2006). Pd30Pt17.5Cu32.5P20 alloy with low critical cooling rate of 0.067 K/s. *Appl. Phys. Lett*. 88: 121908-1–121908-

Park, E. S., Lim, H. K., Kim, W. T. and Kim, D. H. (2002).The effect of Sn addition on the glass-forming ability of Cu-Ti-Zr-Ni-Si metallic glass alloys *J. Non-Cryst. Solids* 298 15

Peker, A. (1994). *Formation and characterization of bulk metallic glasses. Dissertation (Ph.D.), California Institute of Technology*.

Peng, W., and Zang Y.(2010)**.** Microalloying of Ytrrium in Zr-based Bulk Metallic Glasses, *Progress in Materials Science, Volume 21, Issue 1, February 2011, Pages 46–52.*

suction casting into copper mold. *Mater. Trans., JIM* 36: 1184–1187.

Suryanarayana, C. and Inoue, A.(2011). Bulk Metallic Glasses, *CRC Press*.

Telford, M. (2004) The Case for Bulk Metallic Glasses

Tamura, T., Amiya, K., Rachmat, R.S., Mizutani, Y., and MiwaK. (2005).Electromagnetic vibration process for producing bulk metallic glasses. *Nat.Mater*. 4: 289–292.

Turnbull, D. (1974). Amorphous solid formation and interstitial solution behaviorin metallic alloy systems. *J. Phys. Colloq*. 35: C4-1–C4-10

Yokoyama, Y., Fukaura, K., Inoue, A. (2002). Cast Structure and Mechanical Properties of Zr-Cu-Ni-Al Bulk Glassy alloys

CURRICULUM VITAE

Name Surname: Doğa BİLİCAN

Place and Date of Birth: İstanbul, 26/06/1990

e-mail: bilicando@itu.edu.tr

EDUCATION:

B.Sc.: Istanbul Technical University

Metallurgical and Materials Engineering